学位申請論文

諏訪　浩

学位申請論文

Focusing Mechanism of Large Boulders to a Debris-Flow Front

土石流先端への大岩塊の集中機構

諏訪　浩

Hiroshi SUWA

主論文

Focusing Mechanism of Large Boulders to a Debris-Flow Front

Hiroshi Suwa

Disaster Prevention Research Institute, Kyoto University, Uji, Kyoto 611, Japan.

Abstract

Observations of debris flows at the Kamikamihori valley on the eastern slope of Mt.Yakedake in the Japan Alps show quantitatively that many large boulders would concentrate at the frontal part of debris flows, and that the size of the largest boulder is nearly equal to the maximum flow depth.

According to a well-circulated hypothesis, this focusing phenomena is due to a combination of an inverse grading process and higher velocity at the upper layers of a flow. Two types of experiments showed that the inverse grading process may occur due to the effects of kinetic sieving and dispersive pressure depending on experimental conditions. However these effects were unexpectedly small. Furthermore, the effect of upward motion of the largest boulder whose diameter is nearly equal to the flow depth is rather minor.

Results of model experiments of debris flows using particle mixtures of three sizes with water on a sloping channel showed not only a clear focusing of larger particles to a flow front, but also a lack of incorporation of large particles into the rear part of the flow. A test comparing the velocity of particles of three different sizes in a bore water flow showed that larger particles would soon attain a higher velocity and approached the bore front faster than did smaller particles.

A theoretical model analysis of selective entrainment of boulders by a flow due to their size difference concluded that the larger size ratio of an overlain boulder to basal boulder promotes an easier pivoting condition for the overlain boulder. Another theoretical motion analysis of a boulder in a bore flow

on a steep valley slope of upper reach showed that the larger a boulder is, the higher velocity exceeding the bore-front velocity the boulder attains, so that a larger boulder can catch up with the bore front faster. In summary, a larger boulder can start faster than a smaller one, and it attains a higher velocity in the flow so as to focus to the bore front.

Key Words: Debris flow, Frontal focusing, Large boulder, Selective entrainment, Size segregation

Introduction

Many large boulders usually accumulate at the frontal part of debris flows. In particular, a few remarkable boulders of the largest size, whose diameters are nearly equal to the flow depth, are found at the very fronts of debris flows in almost every case at the field observation site of Mt.Yakedake. Debris flows pose catastrophic hazards due to their large destructive forces. This is mainly due to this distinctive boulder focusing and accumulation phenomena, so that much effort has been paid by many researchers to clarify this focusing mechanism.

This focusing phenomena formerly was well-known only qualitatively, but recently the actual measurements by field observations of debris flows (Okuda et al.,1976,1977; Suwa et al.,1984, 1985a,b,1986; Ishikawa,1985; Pierson,1986) confirmed this focusing phenomena quantitatively.

On the other hand, many experimental studies (Takahashi,

1980; Hirano et al.,1981;Hashimoto et al.,1983; Suwa et al.,1984, 1985a,1986;Yamano et al.,1985) discussed this focusing phenomena. Although Hirano et al.(1981) experimentally showed lack of incorporation of large particles into the frontal part of a flow, other researchers followed Bagnold(1968), who suggested that relatively large particles drift upwards (inverse grading), and since the upper surface moves fastest, the large particles drift towards the front of the flow. Takahashi(1980) applied Bagnold's (1954) dispersive pressure to his model to explain the upward motion of a large particle in a grain flow. Suwa et al. (1984,1985a,1986) and Yamano et al.(1985) considered kinetic sieving or percolation of particles, which were reviewed by Naylor(1980), for the explanation of upward motion of large particles. Hashimoto et al.(1983) discussed the upward motion of large particles with their concept of two forces from contact and from collision between particles. Although Suwa et al.(1982,1983) found an inverse grading structure among debris-flow deposits on a fan, they couldn't judge whether that structure was the frozen remains of the inverse grading structure of flowing debris or was a result of a special depositional process of a debris flow on account of a lack of visual record during the stopping stage.

None of the above mentioned analyses actually evaluated the upward velocity of larger particles or the focusing process of the largest boulder whose size is nearly equal to the flow depth. In order to explain this focusing mechanism, a series of model experiments of debris flows and of new motion analyses on a boulder in a flow have been executed from a viewpoint different from those of the past.

Field Data from the Debris-Flow Observations

Field observations of debris flow have been carried out since 1970 at the Kamikamihori valley of Mt.Yakedake in the Japan Alps by our group of the Disaster Prevention Research Institute in cooperation with the Matsumoto Sabo Construction Office in the Ministry of Construction. The emphasis of measurement was initially on the flow stage of debris flows (Okuda et al., 1976,1977,1980,1981;Suwa et al.,1973a,1984,1985b,1986) during the two periods from 1970 to 1975 and from 1983 to 1986, secondly on the occurrence stage (Okuda et al.,1979) from 1976 to 1978 and from 1987, and thirdly on the deposition stage (Suwa et al.,1982,1983) from 1979 to 1982, respectively. For the measurement of the flow stage of a debris flow, an automatic, remote-controlled observation system with two types of speedometers, video-camera recording and time-lapse photography was contrived by us and is being used at the main observation site near the dam No.6 upper as found in Fig.1, to obtain velocity, depth, flow rate and debris composition data for many debris flows. Since 1970, 60 debris flows have occurred in this valley. Of those flow stage data for 46 flows were successfully collected, providing useful information not only for fundamental studies of debris flows but also for practical countermeasures against debris flow hazards.

In the results from the above observations, several common characteristics can be found in the relationship between the composition of debris material and hydraulic values of the flow. These characteristics can be seen clearly in the data for the first surge of the 1985 July 21 debris flows. Three series of

35 mm pictures of this flow are shown in Photo 1 - 3. Three 35 mm cameras have been used for photographing the flows at the same point from different angles to measure material composition and an exact shape in three-dimensions. Photo 1 shows a frontal view of a flow from which cross sectional area of the flow can be extracted. A lateral-angle picture, Photo 2, shows a typical steep slope of the debris-flow front and a remarkable accumulation of many big boulders at the frontal part (head) of the flow.

A vertical-angle picture, Photo 3, shows a boulderly and muddy top surface of the flow. The first two views of Photo 3 show an important fact that the finer matrix slurry is absent in the interstices of large boulders at a frontal edge zone of the flow. For later discussion, note the slurry absence at the edge front and the continuous transition from a highly boulderly zone to muddy flow head (Suwa et al.,1984,1985a,b,1986). Concerning this property of debris flows, Ishikawa(1985) also observed a frontal accumulation of large boulders in a debris flow at the Name river, which is a tributary of the Kiso river in Japan, while Pierson(1986) found that the muddy slurry did not fill up the boulderly interstices of the front edge of debris flows on the slope of Mount St.Helens in USA.

Time changes in the content and the size distribution of gravel particles whose diameters are larger than 10 cm were extracted from the same series of Photo 3, and they are shown in Fig.2 along with the time change of hydraulic values of the flow. In this diagram, content of gravel means the areal percentage of the picture occupied by gravels. The largest diameter of each

gravel particle on the picture was picked for each nominative diameter instead of adopting mean diameter to avoid an underestimation due to the hiding effect of immersion of gravel in muddy slurry or to the overlapping of gravels each other. Fig.2 distinctively shows focusing of large boulders to the flow front and a piling up of a huge amount of boulders in the flow head which gave a very massive shape to the flow front. Besides the frontal focusing of large boulders, there is another significant fact to be observed in Fig.2; the sizes of the several 'biggest' boulders are larger than or nearly equal to the flow depth, and those biggest boulders are also concentrated at the flow front.

The frontal part of debris flows have a lower flow velocity than the following part as shown in Fig.2 as a result of two effects. The first is the greater frictional forces between the large boulders and the valley bottom and the other is greater friction between boulders in the local absence of muddy slurry. As a result of this significant change in the mechanical state of flowing debris, peak hydraulic values generally occur sequentially following the order of flow depth, flow rate and surface velocity as found in Fig.2. After the peak in surface velocity, all values gradually diminish. The graph in Fig.2 further shows that the second surge exhibits the same appearance order of peak hydraulic values.

Criticism of Past Explanations of Frontal Focusing by Inverse Grading Process

An original hypothesis by Bagnold(1968) about the focusing mechanism of large boulders to a debris-flow front has been adopted by almost every researcher who thereafter discussed this phenomena. His idea is that the upward motion of relatively large boulders and the higher velocity at the upper layer of the flow cause the frontal accumulation of larger boulders. This upward motion gives a flow an inverse grading structure of gravels which is attributed to either the dispersive pressure effect (Bagnold, 1954,1968; Takahashi,1980,1984) or the kinetic sieving effect (Middleton,1970; Naylor,1980).

Concerning the above explanation, the author proposes his alternative view for the following reasons. Firstly an alternative explanation is necessary for the frontal focusing of 'largest' boulders whose upward motion cannot occur because their diameter is larger than or nearly equal to the flow depth. Secondly, experimental study is necessary to evaluate the effect of inverse grading quantitatively for practical application to large boulders which are also relatively smaller than the flow depth. Accordingly, the following two kinds of experiments were carried out to evaluate the inverse grading effect. One is a vibrating test of a particle mixture to determine size segregation due to kinetic sieving, and the other is a shearing test of a particle mixture for size segregation due to dispersive pressure and kinetic sieving.

Here kinetic sieving means an upward motion of relatively large particles as a result of a percolation (=falling down) of

smaller particles through the interstices of large ones. The effective force due to kinetic sieving is unknown at the present. On the other hand, dispersive pressure, p_d, originates from momentum transfer in the grain flow by the collision of particles in neighbouring layers of different velocity and was expressed

$$P_d = a_i \sigma \lambda f(\lambda) D^2 \left(\frac{du}{dy}\right)^2 \cos\alpha_i \qquad (1)$$

in a two dimensional uniform steady shear flow by Bagnold(1954), where a_i is a constant, σ is the particle density, $\lambda = \{(C_0/C)^{1/3} - 1\}^{-1}$ is the linear concentration of particle in the flow, C_0 is a possible closest volume concentration of particle, C is the volume concentration of particle in the flow, D is the particle diameter, u is velocity of fluid in the main flow direction, y is the coordinate perpendicular to an equal-velocity plane and α_i is an inertial friction angle due to particle collision. According to the equation (1), the dispersive stress appears to push the relatively large particles towards the region of least shear rate.

Size segregation by kinetic sieving is considerd to be generated only if a particle mixture is in a fluidized state where rearrangement of particles is possible in the presence of gravity field. In the first experiment, a vibration test of a particle mixture was executed to evaluate the effect only by kinetic sieving (Suwa et al.,1984,1985a). As a result of this experiment, it was shown that the following two conditions are necessary for kinetic sieving to occur. One is that the maximum acceleration of vibration must exceed a large critical value, 15G, in water which can hardly be generated in a debris flow according to our observation. The other is that a size ratio,

which is defined as a diameter ratio of a large particle to a small one, must exceed a critical value, r_k, which is a certain value between 2 and 3, coinciding with Hayashi's(1970) similar value, 2.5 . On the other hand, rearrangement of particles is always possible in a shear flow of a particle mixture, but the rate of kinetic sieving in such a flow was difficult to evaluate from the results of the vibration test.

Shearing tests of particle mixtures were carried out using a ring-shaped flume (Suwa et al.,1986) to study the size segregation due to the dispersive pressure effect and the kinetic seiving effect with glass particles, and to study the size segregation due to only the former effect with neutrally buoyant particles made of ABS or polystylene plastics. The segregation results of the shear test depended on experimental conditions. The velocity distribution of the shear flow did not agree with those in studies by Bagnold(1968) and by Takahashi(1980), where the shear rate increased with depth. That is, all the shear tests with glass particles showed an almost linear distribution of flow velocity as shown in Fig.3, where a high content of large particles generated an inverse grading structure in the flow, and a low content of large particle resulted in normal grading. In these segregation test, kinetic sieving was possibly present, but dispersive pressure had no effect on the vertical motion of large particles due to the constant shear rate.

Every shear test with neutrally buoyant particles had a convex upward distribution of velocity as shown in Fig.4. In this case large particles drifted upward contrary to the predicted effects of dispersive pressure and in the absence of kinetic sieving due to the neutral buoyancy of the particles in water.

Consequently, although inverse grading may occur under specific conditions and with enough time, a strong inverse grading process was by no means verified. Furthermore, the frontal focusing of the largest boulders cannot be explained by an inverse grading process when the boulder size is nearly equal to the flow depth and when the largest boulders are transported almost continuously contacting the bottom surface. The largest boulders surely run down frequently protruding from the tops of flows in some debris flows. But the author does not think that this occasional saltation is a major cause of the frontal focusing of the largest boulders. Therefore more experiments to test the direct process of frontal focusing of large boulders were needed.

Tests of Movement of Large Particles towards a Bore Front on a Sloping Channel

The structure of a sloping flume is shown in Fig.5. In the experiments, mixtures of the test particles were distributed uniformly over the reach between x=50 and 470 cm on the flume whose surface was laid with a woven net of 1 mm wire in the pattern of 1 cm regular square grid for the particles not to slip on the bottom surface. When the gate of a water tank at the upper end of the flume was released, a water bore ran downward entraining the particles successively to generate a typical bore flow of particle mixture very similar to a real debris flow. Two video cameras were used to take pictures from vertical and

lateral angles to obtain velocity and flow depth.

In the first experiment, a particle mixture of three different sizes was utilized. The diagram of particle content of each size in Fig.6 shows a distinctive concentration of large particles towards the flow front. The bottom diagram shows the time change of flow depth and the distribution of flow velocity at the times of 0.48, 0.71, 0.95, 1.41 second. Specific attention should be paid to the velocity distributions, which are almost linear or sigmoidal, contrary to that of the dilatant flow model of Bagnold(1968) and Takahashi(1980). A sigmoidal velocity profile, which has two layers of low shear rate near the top surface and near the bottom boundary, can be seen at the time 0.95 second just similar to the profile by Tsubaki et al.(1982).

The second experiment tested the process causing lack of incorporation of a large particles into the rear part of flows. The initial distribution of particles was the same as that in the experiment of Fig.6 except that the large particles were divided into four equal weight groups and painted in four different colors for observation. The four groups were set individually on four sections of equal length on the sloping reach. As a result of this test, it was found that the large particles were moved towards the flow front preserving the initial arrangement order of large particle in the four groups, as shown in Fig.7. This result means that the large particles took the arrangement position in the order of the entrainment and accumulated at the frontal part of the flow in that order, because newly entrained large particles would tend not to be incorporated in the flow due to the repulsive action of collision with other particles already collecting in the flow front.

A series of third tests were carried out to observe whether frontal focusing of particles would occur using a single size of particles. It was also found that the frontal focusing of particles was generated by the test with particles of every uniform size. Fig.8 shows the result of this test, where a frontal focusing of particles was observed under the condition of the same bore water flow running down over the particle deposits. These results of frontal focusing of single-size particles cannot be explained by the well-circulated theory by Bagnold(1968) which explains frontal focusing of larger particles only in a flow consisting of particles of different sizes. A combination of this result and the former result of the tests with particles of three sizes suggests that the relatively forward location of the larger particle as shown in Fig.6 and 7, should be ascribed to a higher rate of frontal focusing of the larger particle.

Then a fourth test was executed to compare the motion of particles of different size. Fig.9 shows a result of this experiment with only four particles, and the position of particles in a bore flow is indicated along with the velocity at each measurement position. There was the following tendency in the motion of each particle: just after the entrainment, though two small particles took the most forward position, they could then only achieve a lower velocity than the frontal velocity of the bore. Therefore, the distance between the particle and the flow front would gradually become longer. Similarly although a medium particle achieved a higher velocity and preceded a large particle just after the entrainment, thereafter it was left behind a large particle due to its lower acceleration. Finally,

however, it achieved a high velocity nearly equal to the frontal velocity of the flow. On the other hand, a large particle only achieved a lower velocity and was left behind other particles just after the entrainment, but it soon arrived at the flow front fastest due to its higher acceleration. Afterward it can be seen that the large particle would keep its position at the flow front. Above all, every motion of particles seemed to be controlled by a force balance between the down-slope component of body force (gravity force of particle), a frictional force on the flume bottom, and a drag force by the flow of water acting on each particle. The motion of boulders in a starting stage and running stage in a flow will be theoretically analyzed in the following two sections.

Model Analysis of Selective Entrainment of Boulders by a Flow due to their Size Difference

Recent studies by Komar et al.(1986) on gravel entrainment thresholds in rivers and offshore tidal currents showed that variations in pivoting angles for grain entrainment have significant effects on selective sorting due to grain size and shape. In general, there are debris deposits with boulders of various sizes and shapes accumulating in the valley bottom at a source area of debris flow as shown in Photo 4. When a muddy water flow occurs along such a valley bottom, the boulders will be entrained selectively due to their size and shape differences and also depending on the flow velocity.

First, consider the model of pivoting conditions of a

spherical boulder sitting on basal boulders as shown in Fig.10. There are five kinds of forces acting on the fully submerged sitting boulder in a uniform current: $F_G=(4/3)\pi R^3 \sigma g$ is the gravity force, $F_B=(4/3)\pi R^3 \rho g \cos\theta$ is the buoyancy, $F_D=(1/2)\varepsilon C_D \rho V^2 \pi R^2$ is the drag force, $F_L=(1/2)\varepsilon C_L \rho V^2 \pi R^2$ is the lift force, and the forces at the contact points P and Q, where σ is the density of boulder, ρ the density of muddy water, g the acceleration of gravity, V the flow velocity of fluid, C_D the drag coefficient, C_L the lift coefficient and ε a coefficient of partial sheltering. This ε is similar to that of Ashida et al.(1977) in their study of the critical tractive force for gravel.

The critical equilibrium condition for a sitting boulder to pivot and to move downwards can be given by equation (2), considering a balance of the moments around the contact point P in Fig.10. This assumes that the effect of partial sheltering of the sitting boulder by the basal boulders is negligible so that ε is approximately equal to 1,

$$\frac{1}{2}C_D\rho V^2\pi R^3\cos\phi+\frac{1}{2}C_L\rho V^2\pi R^3\sin\phi+\frac{4}{3}\pi R^4\rho g\cos\theta\sin\phi$$
$$=\frac{4}{3}\pi R^4\sigma g\sin(\phi-\theta) \qquad (2)$$

where θ is the slope angle and ϕ the pivoting angle. Equation (2) is rewritten as:

$$Fr^2=F_p(R/r) \qquad (3)$$

where two dimensionless numbers are defined respectively as

$$Fr^2\equiv\frac{V^2}{rg} \qquad (4)$$

$$F_p\equiv\frac{8}{3C_D}\cdot\frac{R}{r}\left\{\frac{\sigma}{\rho}\sin(\phi-\theta)-\cos\theta\sin\phi\right\}\Big/\left(\cos\phi+\frac{C_L}{C_D}\sin\phi\right) \qquad (5)$$

The sitting boulder will pivot and become entrained in the flow

at the instant when the left hand term (same form as square of Froude number) of equation (3) exceeds the right term, which is called the 'pivoting factor' in this paper.

The pivoting angle ϕ defined as in Fig.10 is a function of size ratio R/r which is empirically given as

$$\phi = k(R/r)^{-m} \tag{6}$$

by Li et al.(1986). According to the results of their experiments, the parameters k and m as given in Table 1 depend on the shape of the gravel and the rotational types of pivot. As for the pivot types, saddle rotation means the case where the sitting boulder pivots through the lower saddle between two basal boulders, and the top rotation means the case where the upper one pivots directly over the top of a basal boulder.

Results of the calculation of $F_p(R/r)$ using equation (6) are shown in Fig.11 for the case of the slope angle $\theta = 5^\circ$ and assuming that $C_L/C_D=0.2$, because of the difficulty in evaluating C_L strictly. Values of pivoting factor $F_p(R/r)$ are compared with three examples of Fr^2 value in this figure. The variety of boulder shapes that permit pivoting increases with flow velocity, and it is easier for boulders to pivot with a larger size ratio R/r.

$F_p(R/r)$ for saddle rotation of ellipsoidal gravel is shown in Fig.12 for changes in slope angle. This figure shows that it is easier for a boulder to pivot on a steeper slope. As for angular gravel, pivoting is more difficult because a steeper slope is necessary for the gravel to pivot as shown in Fig.13. A common property in Figs.11,12,13 is that it is easier for a boulder to pivot with larger size ratio. In other words, a larger boulder is able to pivot earlier when the flow velocity of muddy

water is increasing with flow depth.

Fig.14 shows a critical size ratio in which the gravel can pivot without any flow, if the special condition $\theta = \phi$ is satisfied. Using this diagram, the ease of pivoting of boulders with different shapes and different types of rotation can be compared.

However, the boulders in actual debris-flows do not always pivot in the manner described by the rule mentioned above. For example, in the case where a large boulder is buried in a thick deposit of basal boulders, there is no tendency for a boulder to pivot in the order of the size from the larger to the smaller. However, if a muddy water flow runs downward along a valley and selectively entrains larger boulders earlier as mentioned above, and grows into a debris flow, one of the factors promoting the frontal focusing of larger boulders is operating even in the initial stage of debris-flow generation. In this model, it is assumed that all boulders are fully submerged in a flow. A sudden rise of water-stage may be brought about by a positive surge. We experience surges under the condition of heavy rainfall. We call it a "Teppo mizu" in Japanese which means a flash flood . In the field, roll wave trains or temporal natural dams made from small slides of side wall would often break down and cause such floods on valley bottom. Or we can regard a successive rise of water-stage in a short time approximately as a sudden rise of water-stage.

Mechanical Analysis of Large Boulders Focusing to a Bore Front

According to the result of the former section and of the study on initiation of boulder motion by the impact force of a bore-flow front (Suwa et al.,1973b), a boulder on a slope starts its downward motion after it is entrained in a flow. Accordingly we consider the motion of a boulder which is already submerged in a flow and discuss the motion from its start with a simple model that closely corresponds to the conditions of the experiments represented in Fig.8 and Fig.9. The model is used to explain the mechanism for the frontal focusing of large boulders in the motion of debris flows.

We assume a steady advance of a uniform bore as shown in Fig.15, and we perform a force balance on a spherical boulder in the flow. Positive velocities and forces are in the downslope direction. The equation of unsteady motion for the boulder is:

$$\frac{4}{3}\pi R^3\left(\sigma+\frac{\rho}{2}\right)\frac{dv}{dt}=\frac{4}{3}\pi R^3\sigma g\sin\theta-\frac{4}{3}\pi R^3(\sigma-\rho)\mu g\cos\theta + \frac{1}{2}C_D\rho\pi R^2(V-v)|V-v| \tag{7}$$

in which R is the radius of boulder, v is the velocity of boulder, V is the flow velocity and μ is the coefficient of kinetic friction. It is assumed that the effect of the lift force is negligible for the evaluation of the frictional force in the right-hand term of eq.(7). Equation (7) is rearranged to give:

$$\frac{dv}{dt}=G+D \tag{8}$$

in which

$$G\equiv\frac{\sigma}{\sigma+\rho/2}g\sin\theta-\frac{\sigma-\rho}{\sigma+\rho/2}\mu g\cos\theta \tag{9}$$

and

$$D\equiv\frac{3C_D}{8R}\cdot\frac{\rho}{\sigma+\rho/2}(V-v)|V-v|=C(V-v)|V-v| \tag{10}$$

where $C\equiv 3C_D\{\rho/(\sigma+\rho/2)\}/(8R)$. Here G is a term combining gravity

and friction forces independent of the radius R, and D is a drag-force term, which decreases in inverse proportion to R.

We analyze the motion of a boulder using a flow chart, which embodies 5 stages as shown in Fig.15. In the first stage, which represents a steep slope in an upper reach of a valley bottom, a resting boulder begins to move and accelerates to approach the flow velocity, V_u. In the second stage, also on the steep slope, the boulder accelerates to approach a terminal velocity, which exceeds V_u. In the third stage, after arriving at a gentle slope in a lower reach, the boulder decelerates to approach the flow velocity, V_l. Then, in the fourth stage, also on the gentle slope, the boulder further decelerates to approach a terminal velocity less than V_l or to cease motion. Finally, a fifth stage corresponds to a process in which, at the end of the first stage, the boulder runs onto the gentle slope from the steep slope before attaining the flow velocity V_l, it then approaches a terminal velocity below V_l or ceases motion.

The motion analysis in each stage is as follows, making frequent references to Fig.15 and Table 2 & 3. In this analysis different values of flow velocity V_u and V_l are assumed on the upper and lower reaches respectively, because an approximately constant velocity of flow is attained by a bore in a short distance on a constant slope as seen in Fig.9.

Stage 1: Substituting the velocity of the boulder, v, from the definition of a velocity deficiency of a boulder (that is $u \equiv V_u - v$) for v in eq.(8) yields:

$$\frac{du}{dt} = -G - C u^2 \qquad (11)$$

Solution of equation (11) on the initial condition v=0 namely

$u=V_u$ at time t=0 is:

$$u=\sqrt{\frac{G}{C}}\tan\left\{\tan^{-1}\left(\sqrt{\frac{C}{G}}\,V_u\right)-\sqrt{GC}\,t\right\} \qquad (12)$$

Putting u=0 in eq.(12) gives the time τ_1

$$\tau_1=\frac{1}{\sqrt{GC}}\tan^{-1}\left(\sqrt{\frac{C}{G}}\,V_u\right) \qquad (13)$$

which is necessary for a boulder to attain the flow velocity, V_u. The time τ_1 in field phenomena can be estimated using the assumptions in Table 3 and V_u=10 m/sec according to the observation results at Kamikamihori valley (Okuda et al., 1977, 1979; Suwa et al.,1984,1985c,1986). For example, τ_1=2.8 seconds for a small boulder of radius R=0.1 m, and τ_1=7.0 seconds for a large boulder R=1 m. Because τ_1 is a monotonically increasing function of the radius, R, every boulder which initially rested on the slope would easily attain the flow velocity V_u in a very short time.

Stage 2: Putting v from the definition formula of a velocity excess of the boulder (that is $u\equiv v-V_u$) into v in eq.(8), we get a slightly different equation of motion:

$$\frac{du}{dt}=G-Cu^2 \qquad (14)$$

using the initial condition u=0 at t=0, solution of the differential eq.(14) becomes:

$$u=\sqrt{\frac{G}{C}}\tanh\left(\sqrt{GC}\,t\right) \qquad (15)$$

In this stage, the velocity of a boulder v gradually approaches a terminal velocity $V_u+\sqrt{G/C}$ from the initial velocity V_u. Putting $u=0.95\sqrt{G/C}$ in eq.(15) gives the time τ_2

$$\tau_2=\frac{1}{\sqrt{GC}}\tanh^{-1}0.95 \qquad (16)$$

which is necessary for a velocity excess u of the boulder to attain 95 % of the final value $\sqrt{G/C}$. The velocity excess u=1.3 m/sec is evaluated with the time τ_2=1.4 seconds for a boulder of radius R=0.1 m, and the velocity excess u=4.8 m/sec with τ_2=5.3

seconds for R=1 m. The larger boulder attains a higher terminal velocity because u is approximately proportional to $\sqrt{R}$ due to the tending of $\tanh(\sqrt{GC}t)$ to 1. And the attaining time τ_2 is very short because τ_2 is a monotonically increasing function of R. Consequently, there is a very significant feature about the motion of boulders in a bore flow on a steep slope: the larger boulders can approach the front of the flow faster than can smaller boulders, owing to a higher terminal velocity, which is much larger than the flow velocity, V_u.

Although a large boulder might tend to precede the bore front just after it caught up to the front, the boulder cannot actually precede the front. This is true because outside the flow, the effect of a large frictional force on the boulder due to the lack of buoyancy in muddy water (density of air ρ is negligible in eq.(8)) makes the boulder decelerate.

These special features of a large boulder in motion already been observed empirically as shown in Fig.9; faster arrival of larger particles at the flow front is seen at a distance of 210 cm from the starting point, and retaining of a large particle at the flow front is seen at the section between 210 cm and 410 cm. On the other hand, newly entrained boulders, especially larger ones, would tend not to be incorporated in the flow because of the repulsive action of collision with other boulders already having collected at the flow front. This was seen in the experiment shown in Fig.7. Retention of those boulders at a flow front forms a boulderly frontal part of a debris flow in which the muddy slurry is almost absent, as shown in Photo 3.

Stage 3: Substituting v from a velocity excess of the

boulder (that is $u \equiv v - V_1$) for v in eq.(8) yields:

$$\frac{du}{dt} = -|G| - C u^2 \tag{17}$$

Solution of equation (17) using the initial condition $u = v_0 - V_1$ at t=0 is:

$$u = \sqrt{\frac{|G|}{C}} \tan\left[\tan^{-1}\left\{\sqrt{\frac{C}{|G|}}(v_0 - V_l)\right\} - \sqrt{|G|C}\, t\right] \tag{18}$$

Putting u=0 in eq.(18) gives the time τ_3:

$$\tau_3 = \frac{1}{\sqrt{|G|C}} \tan^{-1}\left\{\sqrt{\frac{C}{|G|}}(v_0 - V_l)\right\} \tag{19}$$

which is necessary for a boulder to decelerate and to attain the smaller flow velocity V_1 on the gentle slope of a lower reach. Suppose the terminal velocity $V_u + \sqrt{G/C}$ has been attained by the boulder in the end of Stage 2, then using Table 3, τ_3=2.4 seconds for a boulder of radius R=0.1 m, and τ_3=17.6 seconds for R=1.0 m. In this way, every boulder will decelerate to the same flow velocity in a short time soon after its arrival at a gentle slope from the upper steep slope.

Stage 4: Putting v from a velocity deficiency (that is $u \equiv V_1 - v$) into v in eq.(8), we get an equation of motion:

$$\frac{du}{dt} = |G| - C u^2 \tag{20}$$

On the initial condition u=0 at t=0, we obtain a solution of eq.(20):

$$u = \sqrt{\frac{|G|}{C}} \tanh\left(\sqrt{|G|C}\, t\right) \tag{21}$$

This solution represents two alternative cases as shown in Fig.15. If the final velocity deficiency $\sqrt{|G|/C}$ is smaller than V_1, the velocity v will gradually approach a terminal velocity $V_1 - \sqrt{|G|/C}$. If, on the other hand, the value of $\sqrt{|G|/C}$ is larger than V_1, the boulder will stop its motion at the time $\tau_{4(2)}$

$$\tau_{4(2)} = \frac{1}{\sqrt{|G|C}} \tanh^{-1}\left(V_l \Big/ \sqrt{\frac{|G|}{C}}\right) \tag{22}$$

Putting $u = 0.95\sqrt{|G|/C}$ in eq.(21) gives the time $\tau_{4(1)}$

$$\tau_{4(1)} = \frac{1}{\sqrt{|G|C}} \tanh^{-1} 0.95 \tag{23}$$

which is necessary for a velocity deficiency of the boulder u to attain 95 % of the final value $\sqrt{|G|/C}$. While a velocity deficiency u=2.3 m/sec is predicted for the example at $\tau_{4(1)}$=21.7 seconds for a boulder of radius R=1 m, another velocity deficiency u=0.3 m/sec is evaluated at $\tau_{4(1)}$=3.0 seconds for R=0.1 m. This means that when the flow velocity on the gentle slope V_1 is smaller than 2.3 m/sec, a boulder of radius R=1 m will stop its motion within 22 seconds, and if V_1 is smaller than 0.3 m/sec, a boulder of R=0.1 m will stop within 3.0 seconds. There is a similar discussion by Ashida et al.(1978) about the terminal velocity of gravel and the flow velocity for critical traction of gravel in the similar situation.

The above results demonstrate a special but natural feature in the motion of many boulders with different sizes: the boulders will stop in the order from larger one to smaller one in a decelerating stage of flow velocity V_1 because $\sqrt{|G|/C}$ is proportional to $\sqrt{R}$. In the field, the larger boulders are observed to be left earlier in the decelerating and depositing stage of debris flow on a fan (Okuda et al.,1979).

Stage 5: Substituting v from a velocity deficiency (that is $u \equiv V_1 - v$) for v in eq.(8) yields:

$$\frac{du}{dt} = |G| - Cu^2 \tag{24}$$

The solution of equation (24) with the initial condition $u=u_0 < V_1$ at t=0 is:

$$\frac{u-\sqrt{|G|/C}}{u+\sqrt{|G|/C}} = \frac{u_0-\sqrt{|G|/C}}{u_0+\sqrt{|G|/C}} \exp\left(-2\sqrt{|G|C}\, t\right) \tag{25}$$

This solution includes two alternative cases for the motion of a boulder as shown in Fig.15 and Table 2; when the final velocity

deficiency $\sqrt{|G|/C}$ is smaller than V_1, the velocity of the boulder will gradually approach a terminal velocity $V_1 - \sqrt{|G|/C}$, and when the value of $\sqrt{|G|/C}$ is larger than V_1, the boulder will stop at a time $\tau_{5(2)}$ as written in Table 2.

Discussion and Conclusion

Frontal focusing of large boulders in debris flows was quantitatively measured during observations of debris flows at the Kamikamihori valley of Mt.Yakedake. According to the results of field observations and experimental tests, it seemed unlikely that the mechanism of such frontal focusing could be explained with a combination of inverse grading and higher velocity in the upper layer in the flow, particulary with respect to the largest boulders in the flow. Kinetic sieveng and dispersive pressure were not sufficient to generate an inverse grading structure in all debris flows. In particular, the velocity distribution in the flow was not suitable to push a relatively large boulder upward with dispersive pressure. Furthermore, the largest boulders cannot make any vertical motion due to dispersive pressure or kinetic sieving in a relatively thin flow. On the other hand, the largest boulders rotate in a relatively thin flow, contacting a bottom surface (Okuda et al.,1976), so that those boulders are expected to climb over small boulders as suggested by Iverson et al.(1987). But such climbing motion has been yet demonstrated neither during our observations nor by the tests on the sloping flume except when particles were entrained.

An experimental test on a sloping flume and a theoretical

analysis were carried out to explain the mechanism of frontal focusing. An analysis of unsteady motion of a spherical boulder in a steadily advancing bore flow predicted that larger boulders would attain a higher terminal velocities in a short time and would catch up with the bore front faster than would smaller boulders. This process was simulated very well by a flume test.

This analysis does not suppose a collective motion of boulders during flow initiation, but rather a surface flow of muddy water which grows and entrains boulders one after another. Then the flow further grows gradually to form a flow of collectively moving boulders, which focus forward soon after entrainment.

There are two successive processes; one is that the larger boulder can start its motion earlier because of selective entrainment, the other is that the larger boulder attains a higher terminal velocity on a steep slope and focuses faster to the front. Moreover, these boulders would form a boulderly front due to boulder retention and to the lack of boulder movement into the body of the flow. The fact that the larger boulder attains a higher terminal velocity, in other words, reveals a very simple and natural aspect of forces which act on the boulder in the flow: body forces (gravity directly and kinetic friction indirectly) act on it in the third power of radius R of the boulder, and surface force (drag) acts in the second power of R. Since the increase of the former force is of course greater than the latter with increasing R, a larger relative velocity is necessary between boulder and flow to get a terminal state in which body forces balance with surface force.

We can understand two processes from the above results. The first one is that, on the upper reach of a valley, there is a very remarkable tendency of erosion in which larger particles have to be entrained more easily, contrary to a popular result of past studies which concludes that smaller particles are removed more easily. This remarkable tendency was explained in the section of the model analysis of selective entrainment, and is surely comfirmed to be one of the fundamental properties in the erosional processes.

The second process is that, on the lower reach of a valley, particularly on a debris-flow fan, there is a natural tendency of sorting, in which size of boulders decreases from the upper part to the lower. This is a result of the depositive processes of debris flows, which corresponds to the second case of the fourth stage in the motion analysis of a boulder: the larger boulders are left earlier on the upper part of a gentle slope than the smaller ones.

Acknowledgment

The author expresses his appreciation to Prof. Setsuo Okuda of Kyoto University for his helpful suggestions and discussions throughout the study. Thanks are due to Dr. Kazuo Okunishi, Mr. Koji Yokoyama, Mr. Tomohisa Manaka of Kyoto University and Mr. Kouichi Ogawa of Kyoto Prefectural University for their fruitful discussion and cooperation in the observation of debris flow at Mt.Yakedake, and to Prof. Takayuki Ishii of Osaka Kyoiku University for his helpful discussion and Mr. Kazuo Oda of Kyoto

University for his cooperation in the experiments. Thanks are also due to Dr. Richard M. Iverson and Dr. Richard LaHusen of U. S. Geological Survey for their critical reviews of the manuscript and useful suggestions.

Observation of debris flow at Kamikamihori valley of Mt.Yakedake has been being executed with the cooperation of the Matsumoto Erosion Control Works of the Ministry of Construction of Japan. Analysis of the visual data of the experiments was technically supported by ADS Co.Ltd. with a image processor PIP-4000. Part of this study is supported through the Grant-in-Aid for Scientific Research on Natural Disaster (No.61025036) of the Ministry of Education, Science and Culture of Japan.

References Cited

Ashida, K., Takahashi, T. and Mizuyama, T. (1977) Study on the Initiation of Motion of Sand Mixtures in a Steep Slope Channel: Shin-Sabo, 103, 6-13 (in Japanese with English abstract).

Ashida, K., Takahashi, T. and Mizuyama, T. (1978) Study on Bed Load Equations for Mountain Streams: Shin-Sabo, 107, 9-17 (in Japanese with English abstract).

Bagnold, R. A. (1954) Experiments on a gravity-free dispersion of large solid spheres in a Newtonian fluid under shear: Proc. Roy. Soc. London, A225, 49-63.

Bagnold, R. A. (1968) Deposition in the Process of Hydraulic Transport: Sedimentology, 10, 45-56.

Hashimoto, H. and Tsubaki, I. (1983) Reverse Grading in Debris Flow: Proc. Jap. Soc. Civil Eng., No.336, 75-84 (in Japanese).

Hayashi, T., Sasano, A., Tsutsumi, M., Kawakita, K. and Ikeda, C. (1970) Segregation in the flow of powder-particles in tapping: Zairyo, 19, 574-578 (in Japanese).

Hirano, M. and Iwamoto, M. (1981) Experimental Study on Front of Debris Flow: Shin-Sabo, 121, 1-7 (in Japanese with English abstract).

Ishikawa, Y. (1985) Debris Flows in the Name River: Shin-Sabo, 136, 24-29 (in Japanese).

Iverson, R. M. and Delinger, R. P. (1987) The physics of debris flows -- a conceptual assesment: IAHS Publ. no. 165 (Proc. Sympo. Erosion and Sedimentation in the Pacific Rim), 155-165.

Komar, P. D. and Li, Z. (1986) Pivoting analyses of the selective entrainment of sediments by shape and size with application to gravel threshold: Sedimentology, 33, 425-436.

Li, Z. and Komar, P. D. (1986) Laboratory measurements of pivoting angles for applications to selective entrainment of gravel in a current, Sedimentology, 33, 413-423.

Middleton, G. V.(1970) Experimental studies related to problem of flysch sedimentation, in Lajoie, J., ed., Flysh Sedimentology in North America: Geol. Soc. Canada Spc. Paper 7, 253-272.

Naylor, M. A. (1980) The origin of inverse grading in muddy debris flow deposits -- a review: Jour. Sed. Petrol., 50, 1111-1116.

Okuda, S., Suwa, H., Nakano, M. and Yokoyama, K. (1976) Synthetic Observation on Debris Flow, Part 2: Annuals of Disas. Prev.

Res. Inst., Kyoto Univ., 19B-1, 385-402 (in Japanese with English abstract).

Okuda, S., Suwa, H., Okunishi, K., Nakano, M. and Yokoyama, K. (1977) Synthetic Observation on Debris Flow, Part 3: Annuals of Disas. Prev. Res. Inst., Kyoto Univ., 20B-1, 237-263 (in Japanese with English abstract).

Okuda, S., Suwa, H., Okunishi, K., Yokoyama, K., Ogawa, K., and Hamana, S. (1979) Synthetic Observation on Debris Flow, Part 5: Annuals of Disas. Prev. Res. Inst., Kyoto Univ., 22B-1, 157-204 (in Japanese with English abstract).

Okuda, S., Suwa, H., Okunishi, K., Yokoyama, K. and Nakano, M. (1980) Observation on the motion of a debris flow and its geomorphological effects: Z. Geomorph. N. F., Suppl.-Bd. 35, 142-163.

Okuda, S., Suwa, H., Okunishi, K., and Yokoyama, K. (1981) Depositional Process of Debris Flow at Kamikamihori Fan, Northern Japan Alps, Trans. Jap. Geomorph. Union, 2(2), 353-361.

Pierson, T. C. (1986) Flow behavior of channelized debris flows, Mount St. Helens, Washington: in Abraham, A. D. ed., Hillslope Processes, Boston, Allen & Unwin, 269-296.

Suwa, H., Okuda, S. and Yokoyama, K. (1973a) Observation System on Rocky Mudflow: Bull., Disas. Prev. Res. Inst., Kyoto Univ., 23, 59-73.

Suwa, H. and Okuda, S. (1973b) Motion of Large Stone at Mudflow Front and Flow Pattern of Mudflow: Annuals of Disas. Prev. Res. Inst., Kyoto Univ., 16B, 425-432 (in Japanese with English abstract).

Suwa, H. and Okuda, S. (1982) Sedimentary Structure of Debris-Flow Deposits, at Kamikamihori Fan of Mt. Yakedake: Annuals of Disas. Prev. Res. Inst., Kyoto Univ., 25B-1, 307-321 (in Japanese with English abstract).

Suwa, H., and Okuda, S. (1983) Deposition of Debris Flows on a Fan Surface, Mt. Yakedake, Japan: Z. Geomorph. N. F., Suppl.-Bd. 46, 79-101.

Suwa, H., Okuda, S. and Ogawa, K. (1984) Size Segregation of Solid Particles in Debris Flows, Part 1: Annuals of Disas. Prev. Res. Inst., Kyoto Univ., 27B-1, 409-423 (in Japanese with English abstract).

Suwa, H., Okuda, S. and Ogawa, K. (1985a) Size Segregation of Large Boulders in Debris Flow: Proc. Inter. Sympo. on Erosion, Debris flow and Disas. Prev. Tsukuba, 237-241.

Suwa, H. and Okuda, S. (1985b) Measurement of Debris Flows in Japan: Proc. 4th Inter. Conf. and Field Workshop on Landslides, Tokyo, 391-400.

Suwa, H. (1985c) Characteristics of Debris Flow and Measurement of Debris-Flow Discharge: Proc. 4th Sympo. on Multi-phase Flow, Tokyo, 157-174 (in Japanese with English abstract).

Suwa, H. and Okuda, S. (1986) Size Segregation of Solid Particles in Debris Flows (Part 2): Annuals of Disas. Prev. Res. Inst., Kyoto Univ., 29B-1, 391-408 (in Japanese with English abstract).

Takahashi, T. (1980) Debris flow in prismatic open channel: Jour. Hydraul. Div. ASCE, 106, 381-396.

Takahashi, T. (1984) Fluid Mechanics on Debris Flow: Jour. Jap. Soc. Fluid Mechanics, 3, 4, 307-317 (in Japanese).

Tsubaki, T., Hashimoto, H. and Suetsugu, T. (1982) Grain Stresses

and Flow Properties of Debris Flow: Proc. Jap. Soc. Civil Eng., No.317, 79-91 (in Japanese).

Yamano, K. and Daido, A. (1985) The Mechanism of Granular Flow of Mixed Diameter Composed Two Diameters: Proc. Jap. Soc. Civil Eng., No.357, 25-34 (in Japanese with English abstract).

Captions

Fig.1. Location of debris flow observations at Kamikamihori valley. R:rain gauge, SS:spatial filter speedometer, RS:radar (Doppler effect) speedometer, 35:35 mm time lapse camera, 8_i:8 mm time lapse camera, V:video camera, S:seismometer, edge arrows:wire sensor for detecting debris-flow arrival.

Fig.2. Change in the composition and in hydraulic factors of debris flow extracted from Photo series 3, a video tape record, and radar speedometer data. Flow depth means the maximum flow depth at one side as seen in Photo 1, which is nearly twice as mean flow depth. After Suwa et al., 1986.

Fig.3. Velocity distribution in a shear flow of glass particles.

Fig.4. Velocity distribution in a shear flow of neutrally buoyant particles.

Fig.5. Sloping flume for test of focusing of large particles to a bore-flow front.

Fig.6. Frontal focusing of large particles in a bore flow of a glass-particle mixture and velocity distribution observed at x=490 cm point. Time=0 indicates when a bore front crossed the center of the view field. 24 mmϕ particle:2.2 kg, 12 mmϕ:4 kg, 4 mmϕ:9.2 kg, water:20 lit., slope angle θ=9°

Fig.7. Distribution of four groups of large particles observed at x=490 cm point, which came from four different sections of the upper depositing reach of particle mixture. Composition of particles and water is same as in Fig.6. Slope angle θ=6.2°.

Fig.8. Frontal focusing of glass particles of uniform size (A: 24 mmϕ particles, B: 12 mmϕ). Change in flow depth observed at x=490 cm point. Amount of particles: 0.56 kg, water: 20 lit., θ=6.2°.

Fig.9. Changes in differential position and velocity of each particle in a bore water flow at three localities at distances 10, 210, 410 cm from the initial position of the particles. Only four particles were set in the flow. L, M, S indicate one 25 mmϕ particle, one 12 mmϕ particle and two 4 mmϕ particles respectively.

Fig.10. Definition sketch for particle entrainment. Four forces operate to rotate a sitting boulder around the pivoting point P. F_G:gravity force, F_B:buoyancy, F_D:drag force and F_L:lift force.

Fig.11. Pivoting factor $F_p(R/r)$ for different shapes of gravel as a function of size ratio R/r and three examples of Fr^2. Pivotable ranges of boulder for r=0.1 m are drawn with bold lines for V=0.5 m/sec and by double lines for V=1 m/sec. Intermediate axial radius is adopted for ellipsoidal gravel and nominative radius for angular gravel.

Fig.12. Pivoting factor $F_p(R/r)$ for ellipsoidal gravel in the case of saddle rotation as a function of R/r for various slope angles.

Fig.13. Pivoting factor $F_p(R/r)$ for angular gravel as a function of R/r for various slope angles.

Fig.14. Critical size ratio, which means the critical pivotable size ratio without any flow, for different shapes of gravel as a function of slope angle θ.

Fig.15. Flow chart connecting the five stages of the motions of a spherical boulder in a steadily advancing and uniform bore flow on a slope. Illustrations show the situations of motion and solutions of their equations of motion. Upper reach, for example, corresponds to the section above the dam No.2 in Fig.1 and lower reach to the section below it.

Table 1. Parameters k and m for equation (6). After Li et al. (1986).

Table 2. Summary of motion analyses of a spherical boulder in five stages as shown in Fig.5.

Table 3. Examples for the physical constants and variables for the calculation of velocity and attaining time of a boulder.

Photo 1. Frontal view of the first surge of debris flows on July 21, 1985, running down over the dam No.6 upper as seen in Fig.1. The number in the photo shows the time interval by seconds from the shuttering time of the first photo.

Photo 2. Lateral view of the same debris flow shown in Photo 1. The channel length in the view field is 12 meters.

Photo 3. Top surface of the same debris flow shown in Photo 1 and 2 just above the dam No.6 upper. Size of the view field is about 4.7 m x 6.6 m. The flow direction is toward the right.

Photo 4. Deposits of different sizes of boulders on the bottom slope in the source area of debris flows at the Kamikamihori valley.

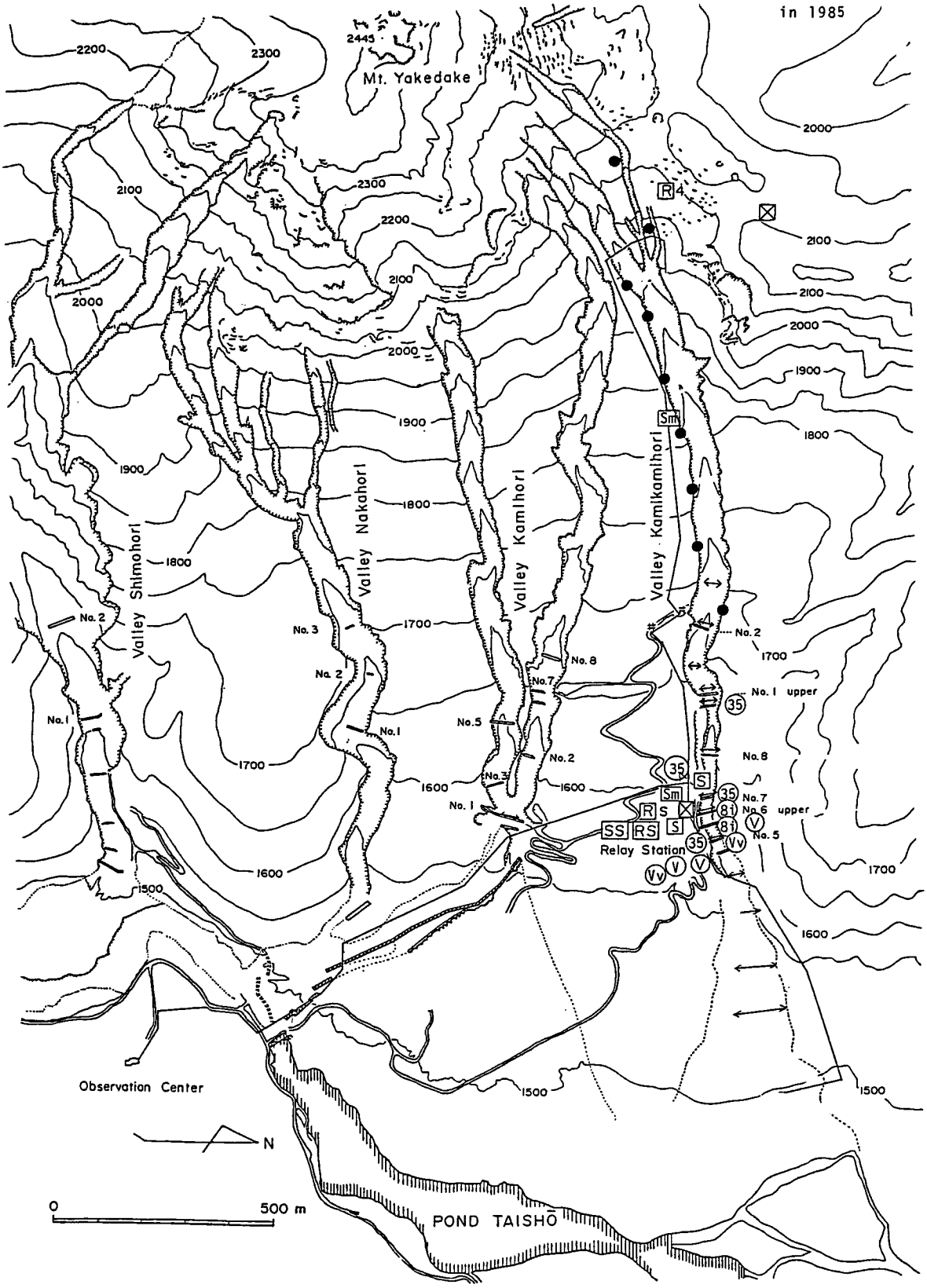

Fig.1. Location of debris flow observations at Kamikamihori valley. R:rain gauge, SS:spatial filter speedometer, RS:radar (Doppler effect) speedometer, 35:35 mm time lapse camera, 8_i:8 mm time lapse camera, V:video camera, S:seismometer, edge arrows:wire sensor for detecting debris-flow arrival.

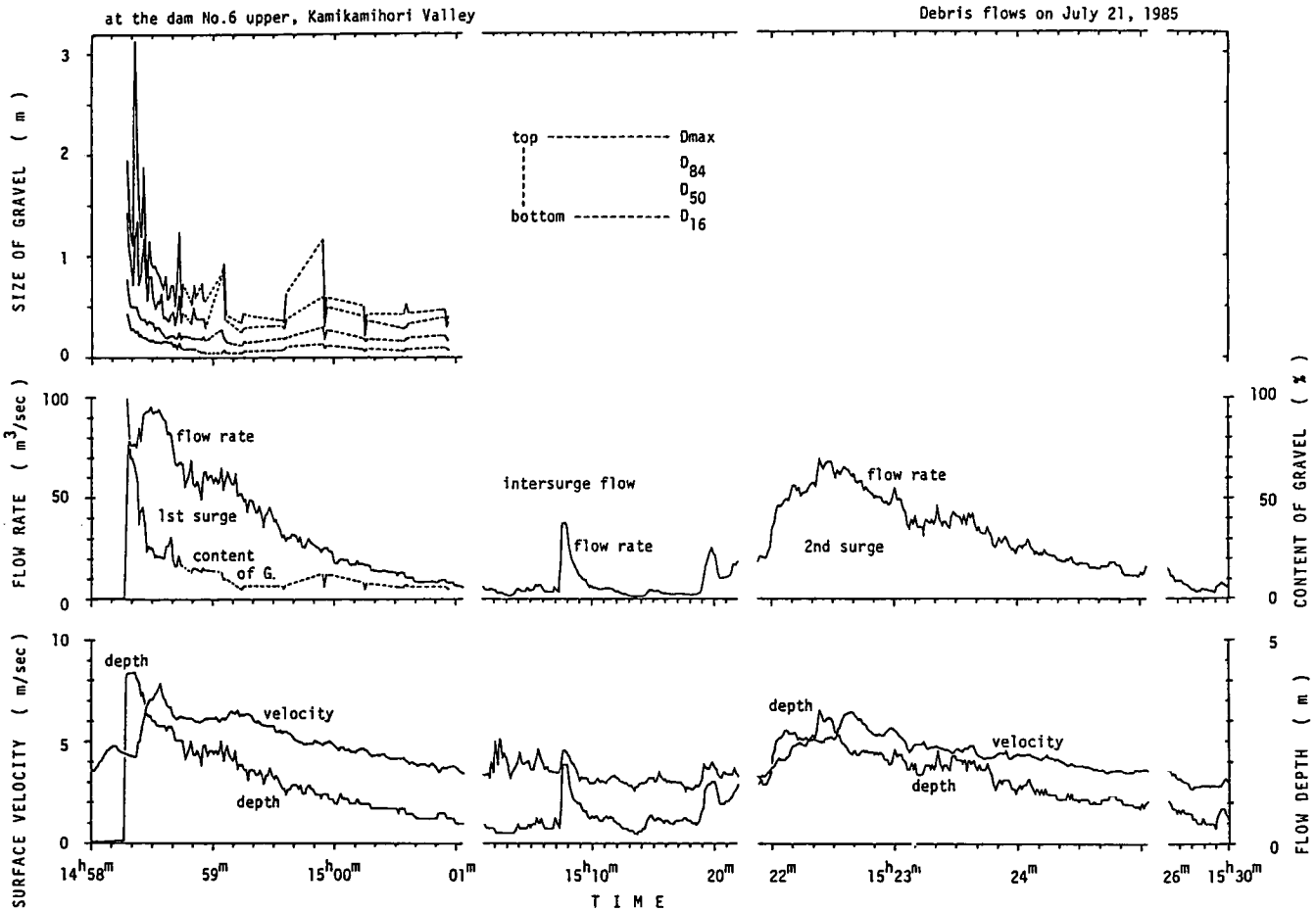

Fig.2. Change in the composition and in hydraulic factors of debris flow extracted from Photo series 3, a video tape record, and radar speedometer data. Flow depth means the maximum flow depth at one side as seen in Photo 1, which is nearly twice as mean flow depth. After Suwa et al., 1986.

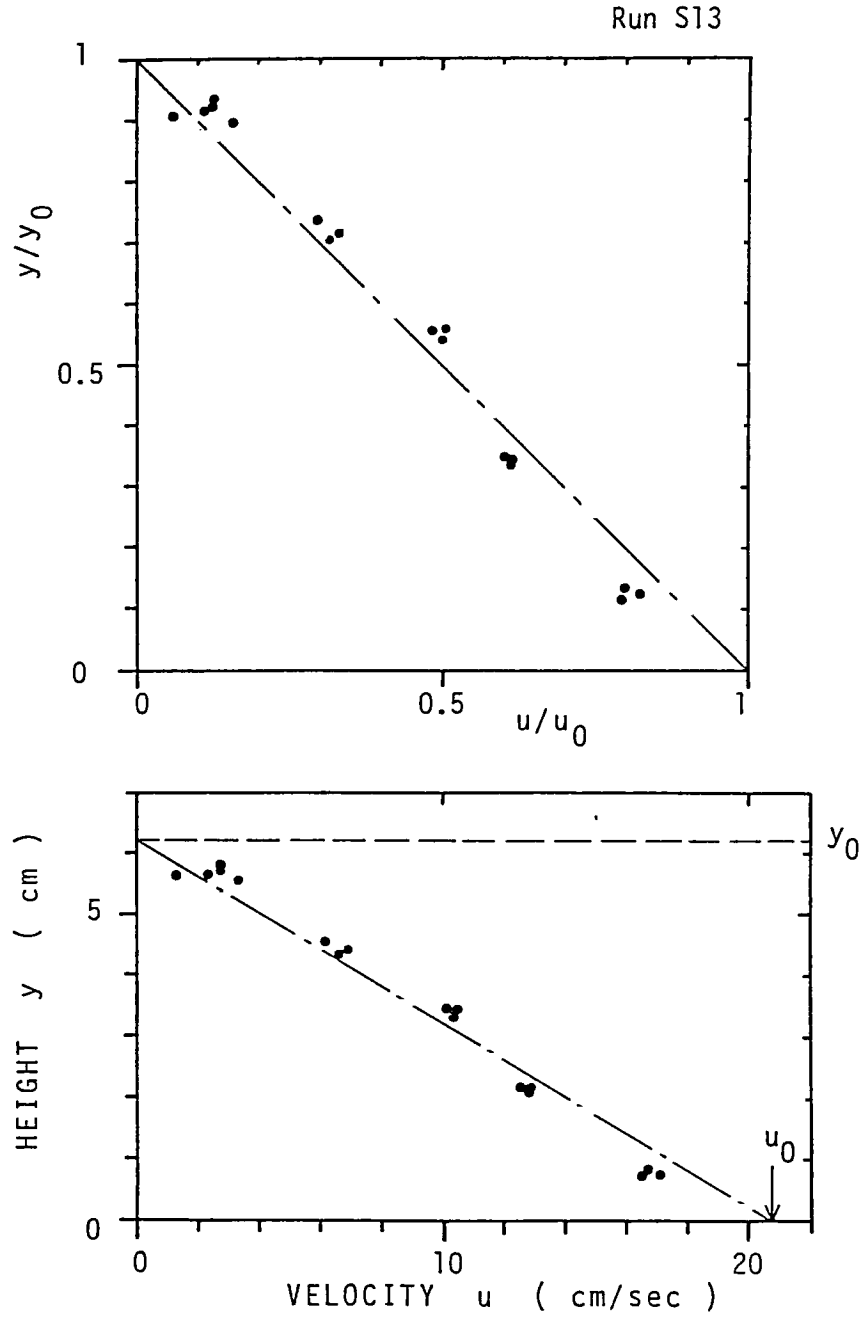

Fig.3. Velocity distribution in a shear flow of glass particles.

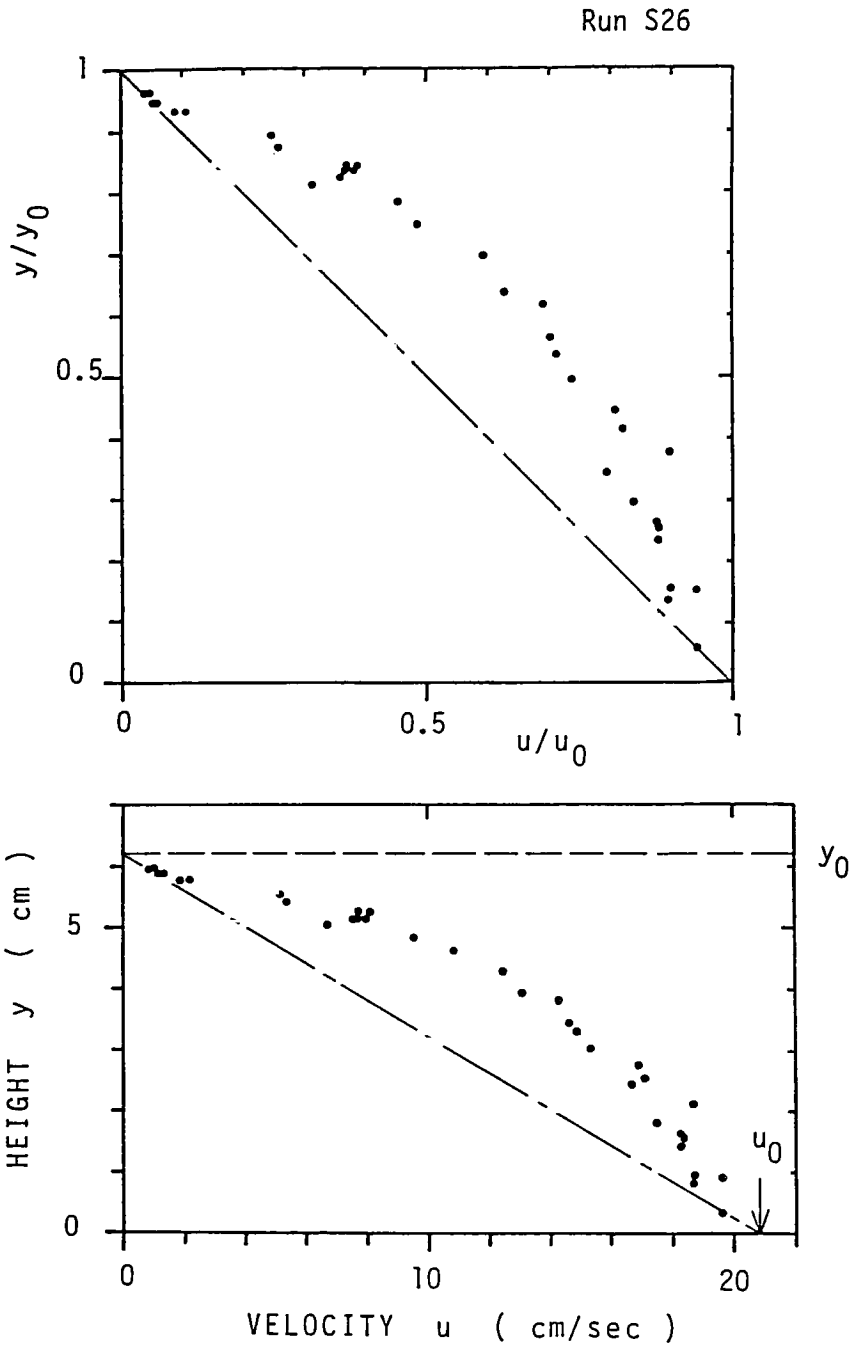

Fig.4. Velocity distribution in a shear flow of neutrally buoyant particles.

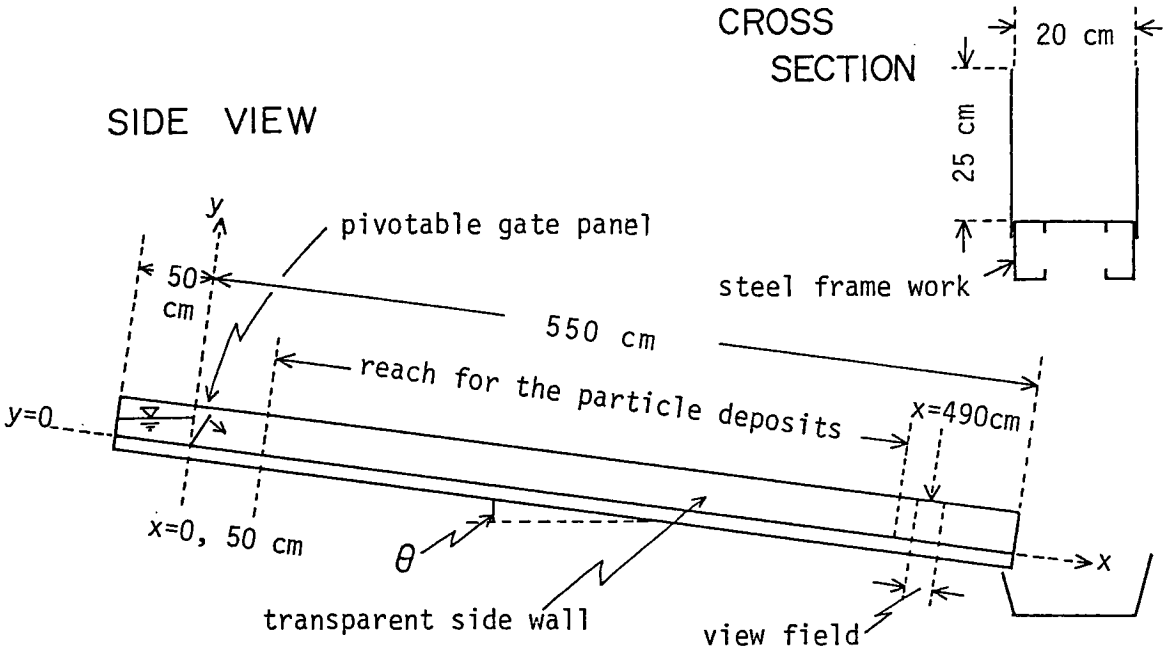

Fig.5. Sloping flume for test of focusing of large particles to a bore-flow front.

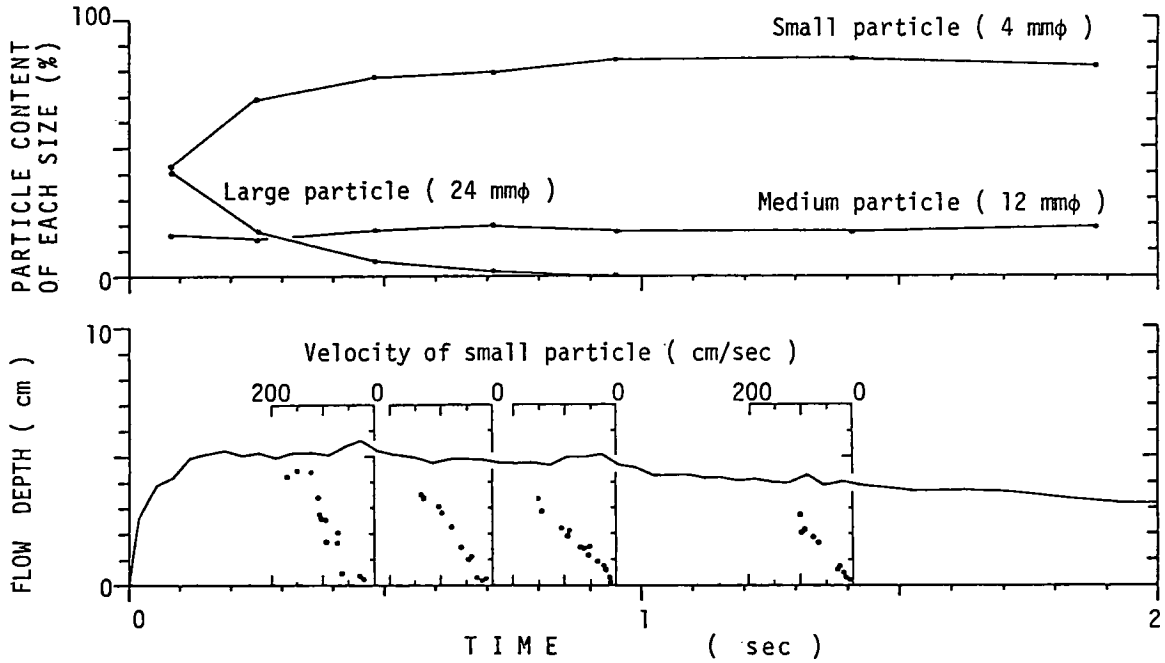

Fig.6. Frontal focusing of large particles in a bore flow of a glass-particle mixture and velocity distribution observed at x=490 cm point. Time=0 indicates when a bore front crossed the center of the view field. 24 mmϕ particle:2.2 kg, 12 mmϕ:4 kg, 4 mmϕ:9.2 kg, water:20 lit., slope angle θ=9°

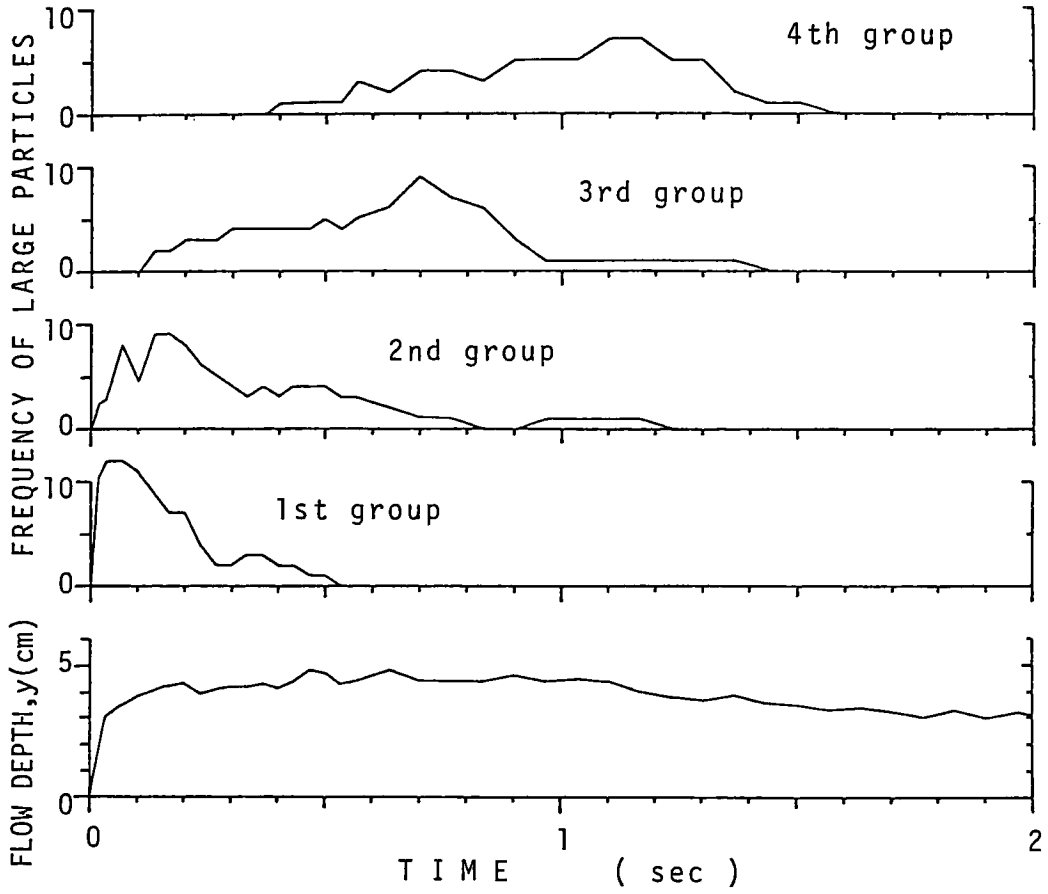

Fig.7. Distribution of four groups of large particles observed at x=490 cm point, which came from four different sections of the upper depositing reach of particle mixture. Composition of particles and water is same as in Fig.6. Slope angle θ=6.2°.

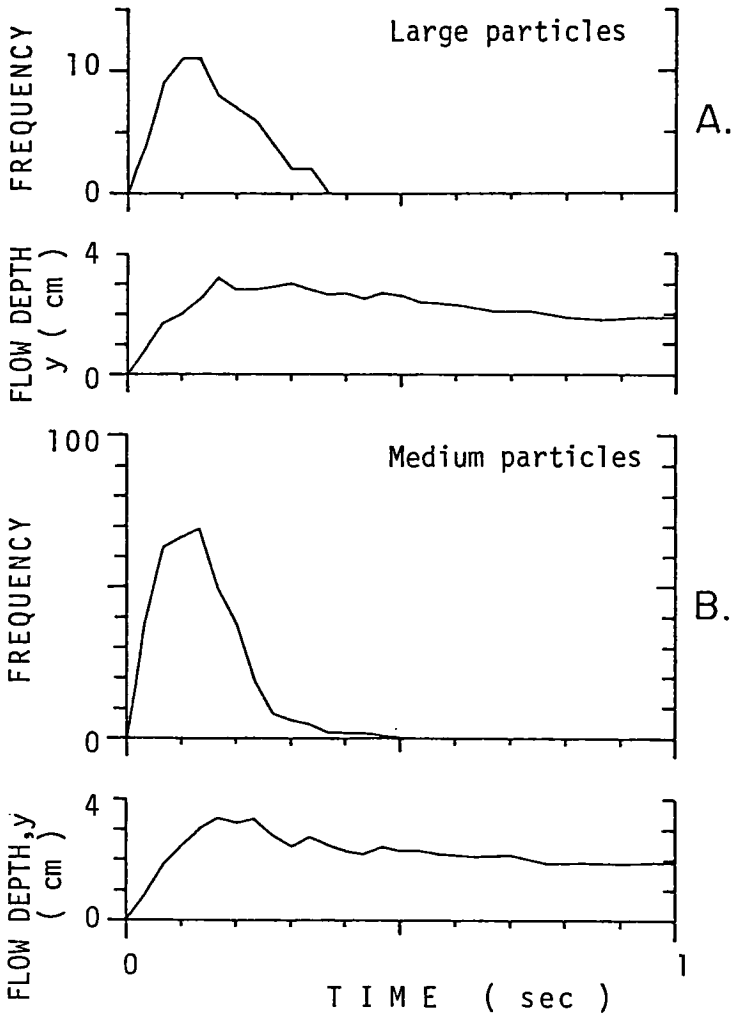

Fig.8. Frontal focusing of glass particles of uniform size (A: 24 mmϕ particles, B: 12 mmϕ). Change in flow depth observed at x=490 cm point. Amount of particles: 0.56 kg, water: 20 lit., θ=6.2°.

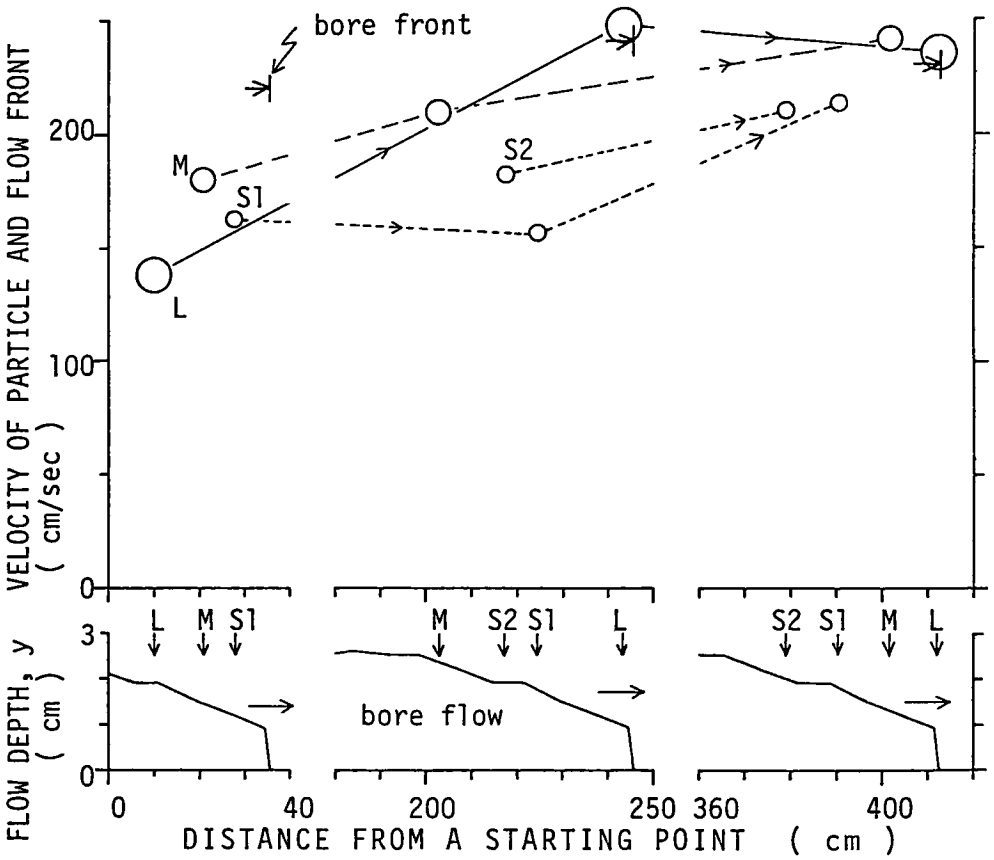

Fig.9. Changes in differential position and velocity of each particle in a bore water flow at three localities at distances 10, 210, 410 cm from the initial position of the particles. Only four particles were set in the flow. L, M, S indicate one 25 mmϕ particle, one 12 mmϕ particle and two 4 mmϕ particles respectively.

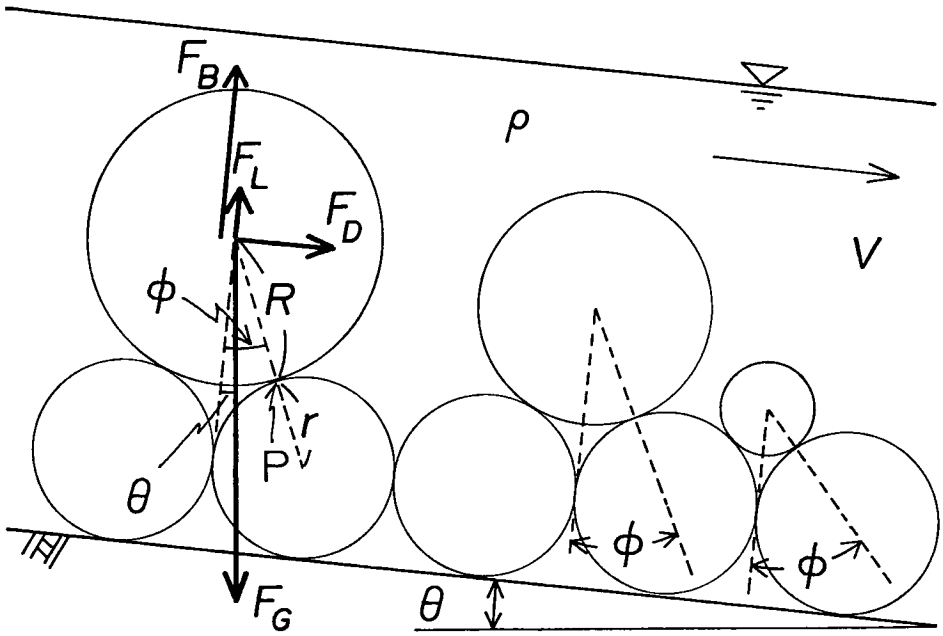

Fig.10. Definition sketch for particle entrainment. Four forces operate to rotate a sitting boulder around the pivoting point P. F_G:gravity force, F_B:buoyancy, F_D:drag force and F_L:lift force.

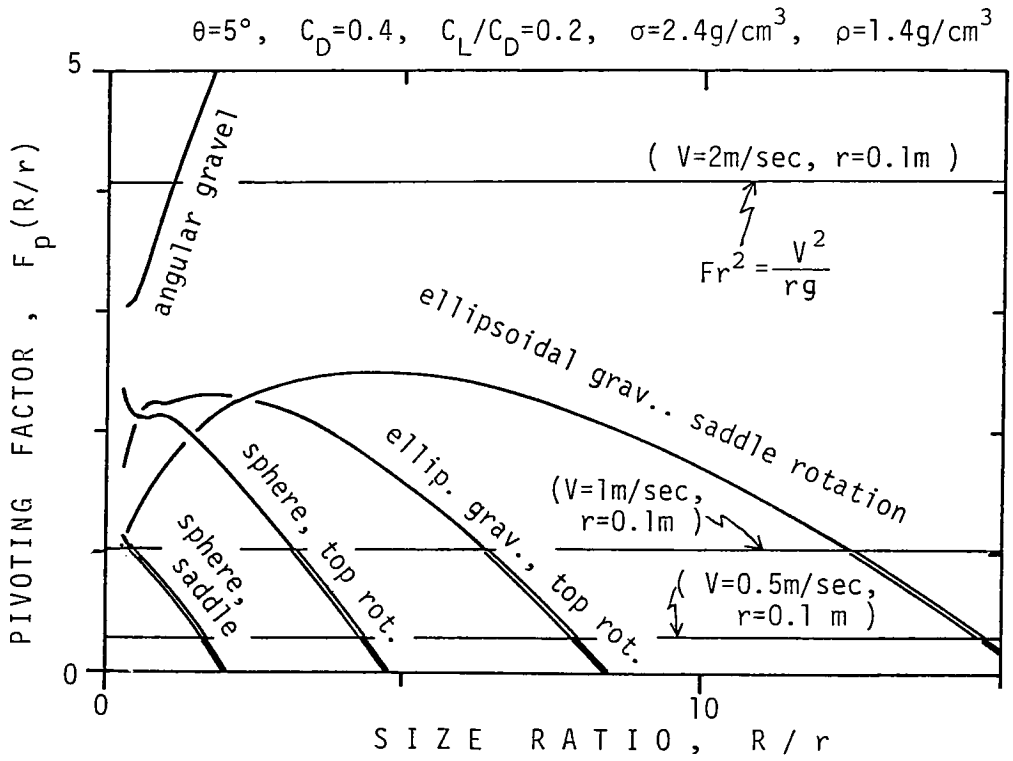

Fig.11. Pivoting factor $F_p(R/r)$ for different shapes of gravel as a function of size ratio R/r and three examples of Fr^2. Pivotable ranges of boulder for r=0.1 m are drawn with bold lines for V=0.5 m/sec and by double lines for V=1 m/sec. Intermediate axial radius is adopted for ellipsoidal gravel and nominative radius for angular gravel.

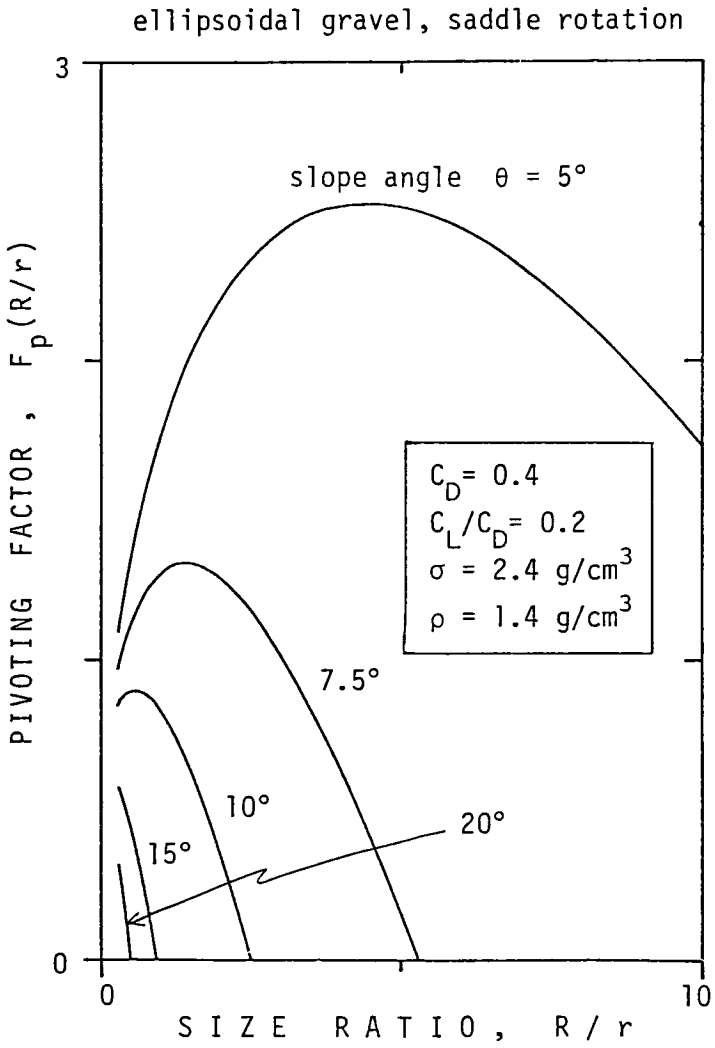

Fig.12. Pivoting factor $F_p(R/r)$ for ellipsoidal gravel in the case of saddle rotation as a function of R/r for various slope angles.

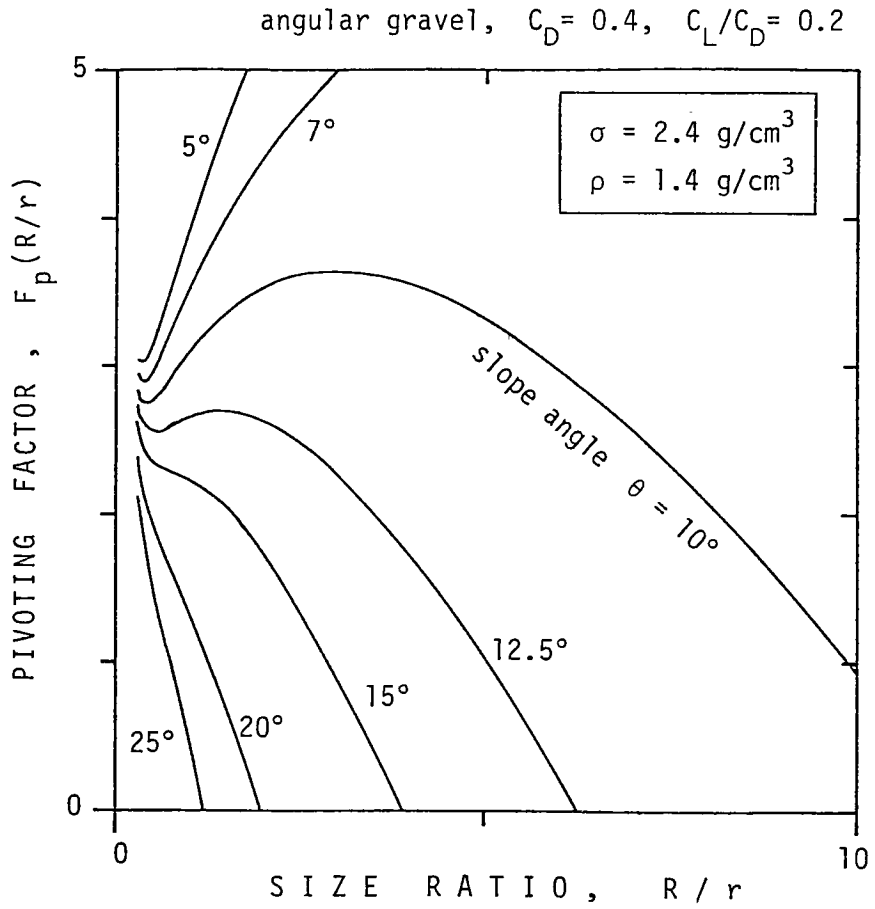

Fig.13. Pivoting factor $F_p(R/r)$ for angular gravel as a function of R/r for various slope angles.

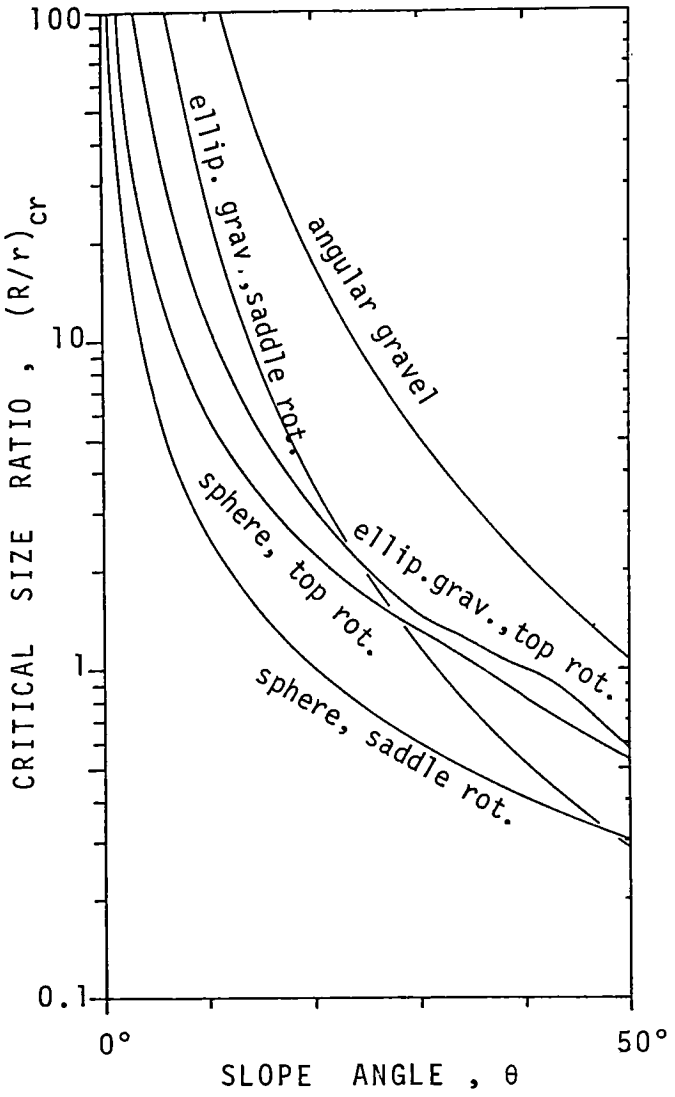

Fig.14. Critical size ratio, which means the critical pivotable size ratio without any flow, for different shapes of gravel as a function of slope angle θ.

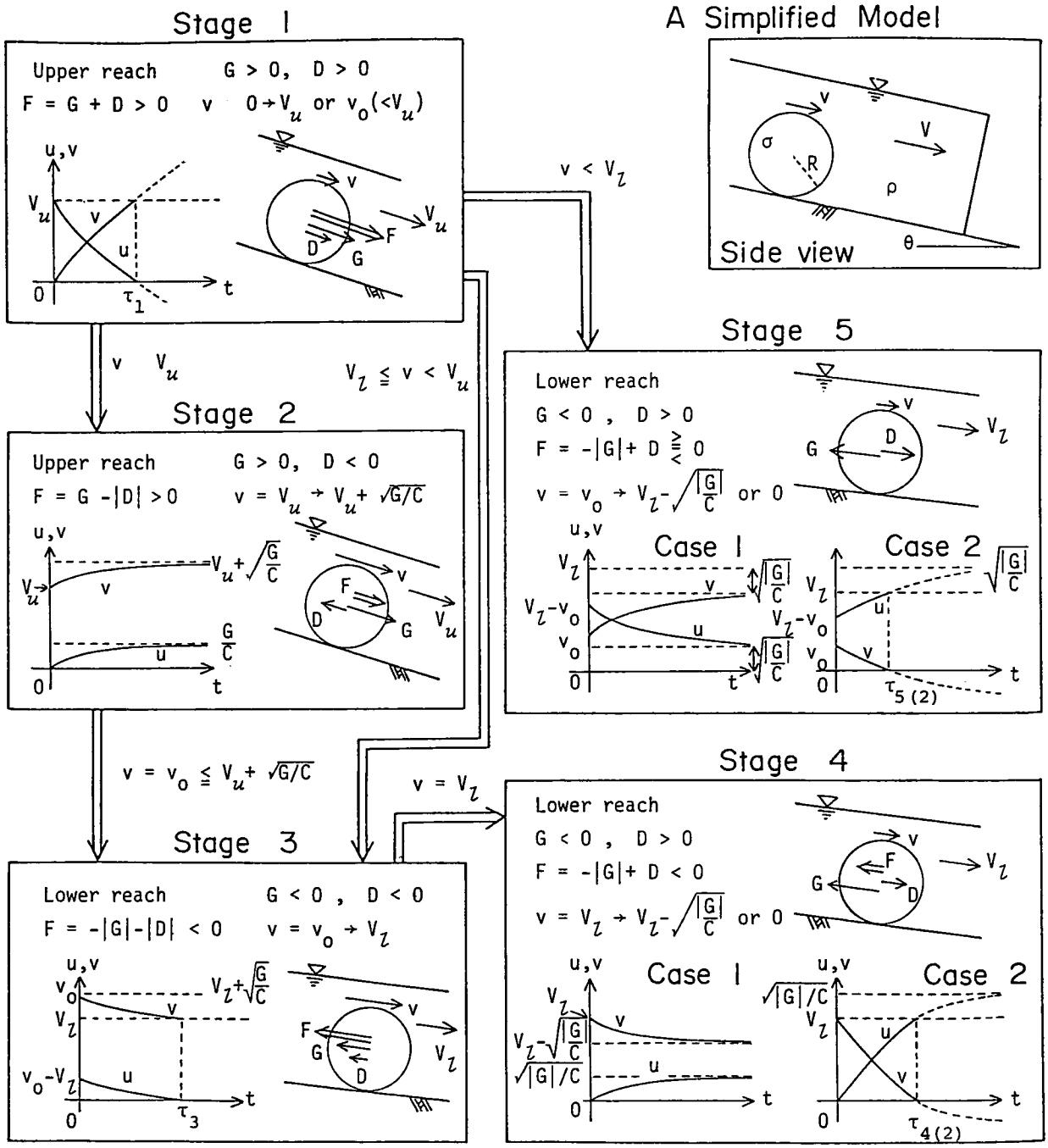

Fig.15. Flow chart connecting the five stages of the motions of a spherical boulder in a steadily advancing and uniform bore flow on a slope. Illustrations show the situations of motion and solutions of their equations of motion. Upper reach, for example, corresponds to the section above the dam No.2 in Fig.1 and lower reach to the section below it.

Table 1. Parameters k and m for equation (6). After Li et al. (1986).

	Rotation	Range of R/r	k	m
Sphere	Saddle	0.3 < R/r	20.4	0.75
	Top	0.3 < R/r < 1	36.3	0.55
		1 ≤ R/r	36.3	0.72
Ellipsoidal gravel	Saddle	0.25 < R/r	31.9	0.36
	Top	0.25 < R/r < 1	42.0	0.32
		1 < R/r	36.8	0.53
Angular gravel		0.3 < R/r	51.3	0.33

Table 2. Summary of motion analyses of a spherical boulder in five stages as shown in Fig.5.

Stage	1	2	3	4	5
Gradient of valley slope	steep (upper reach)	steep (upper reach)	gentle (lower reach)	gentle (lower reach)	gentle (lower reach)
G	+	+	-	-	-
Relative velocity of boulder	deficiency $u \equiv V_u - v$	excess $u \equiv v - V_u$	excess $u \equiv v - V_l$	deficiency $u \equiv V_l - v$	deficiency $u \equiv V_l - v$
D	+	-	-	+	+
Combined force	$G + D > 0$	$G - \lvert D\rvert > 0$	$-\lvert G\rvert - \lvert D\rvert < 0$	$-\lvert G\rvert + D < 0$	$-\lvert G\rvert + D \gtreqless 0$
Equation of motion	$\frac{du}{dt} = -G - Cu^2$	$\frac{du}{dt} = G - Cu^2$	$\frac{du}{dt} = -\lvert G\rvert - Cu^2$	$\frac{du}{dt} = \lvert G\rvert - Cu^2$	$\frac{du}{dt} = \lvert G\rvert - Cu^2$
Initial condition at each stage ($t = 0$)	$u = V_u$ ($v = 0$)	$u = 0$ ($v = V_u$)	$u = v_0 - V_l$ ($v = v_0$)	$u = 0$ ($v = V_l$)	$u = u_0$ ($v = v_0 < V_l$)
Equation of solution	(12)	(15)	(18)	(21)	(25)
v at the final state of each stage	$v = V_u$ at $t = \tau_1$	$v = V_u + \sqrt{G/C}$ at $t = \infty$ $\sqrt{G/C} = \text{const.} \times \sqrt{R}$	$v = V_l$ at $t = \tau_3$	Case 1: for $\sqrt{\lvert G\rvert/C} < V_l$ $v = V_l - \sqrt{\lvert G\rvert/C}$ at $t = \infty$ Case 2: for $\sqrt{\lvert G\rvert/C} > V_l$ $v = 0$ at $t = \tau_{4(2)}$	Case 1: for $\sqrt{\lvert G\rvert/C} < V_l$ $v = V_l - \sqrt{\lvert G\rvert/C}$ at $t = \infty$ Case 2: for $\sqrt{\lvert G\rvert/C} > V_l$ $v = 0$ at $t = \tau_{5(2)}$
Attaining time:	$\tau_1 = \frac{1}{\sqrt{GC}} \tan^{-1}\left(\sqrt{\frac{C}{G}}\, V_u\right)$,	$\tau_3 = \frac{1}{\sqrt{\lvert G\rvert C}} \tan^{-1}\left(\sqrt{\frac{C}{\lvert G\rvert}}(v_0 - V_l)\right)$			
	$\tau_{4(2)} = \frac{1}{\sqrt{\lvert G\rvert C}} \tanh^{-1}\left(V_l / \sqrt{\frac{\lvert G\rvert}{C}}\right)$	$\tau_{5(2)} = \frac{1}{2\sqrt{\lvert G\rvert C}} \ln\left(\frac{u_0 - \sqrt{\lvert G\rvert/C}}{u_0 + \sqrt{\lvert G\rvert/C}} \cdot \frac{V_l + \sqrt{\lvert G\rvert/C}}{V_l - \sqrt{\lvert G\rvert/C}}\right)$			

Table 3. Examples for the physical constants and variables for the calculation of velocity and attaining time of a boulder.

σ = 2.4 g/cm^3	, ρ = 1.8 g/cm^3	
μ_l = 0.6 (for large value)	, μ_s = 0.3	(for small value)
θ_u = 20° (for an upper reach)	, θ_l = 5°	(for a lower reach)
R_l = 1 m (for a large boulder),	R_s = 0.1 m	(for a small boulder)
C_D = 0.4 (for a range of Reynold's number 10^3—— 10^5)		
then		
G_u (for an upper reach)	$G_{u,max}$ = 1.93 m/sec^2	
	$G_{u,min}$ = 1.43 m/sec^2	
G_l (for a lower reach)	$G_{l,max}$ = -0.087 m/sec^2	
	$G_{l,min}$ = -0.44 m/sec^2	
and		
C_{min} = 0.081 m^{-1} for a large boulder (R_l = 1 m)		
C_{max} = 0.81 m^{-1} for a small boulder (R_s = 0.1 m)		

Photo 1. Frontal view of the first surge of debris flows on July 21, 1985, running down over the dam No.6 upper as seen in Fig.1. The number in the photo shows the time interval by seconds from the shuttering time of the first photo.

Photo 2. Lateral view of the same debris flow shown in Photo 1. The channel length in the view field is 12 meters.

Photo 3. Top surface of the same debris flow shown in Photo 1 and 2 just above the dam No.6 upper. Size of the view field is about 4.7 m x 6.6 m. The flow direction is toward the right.

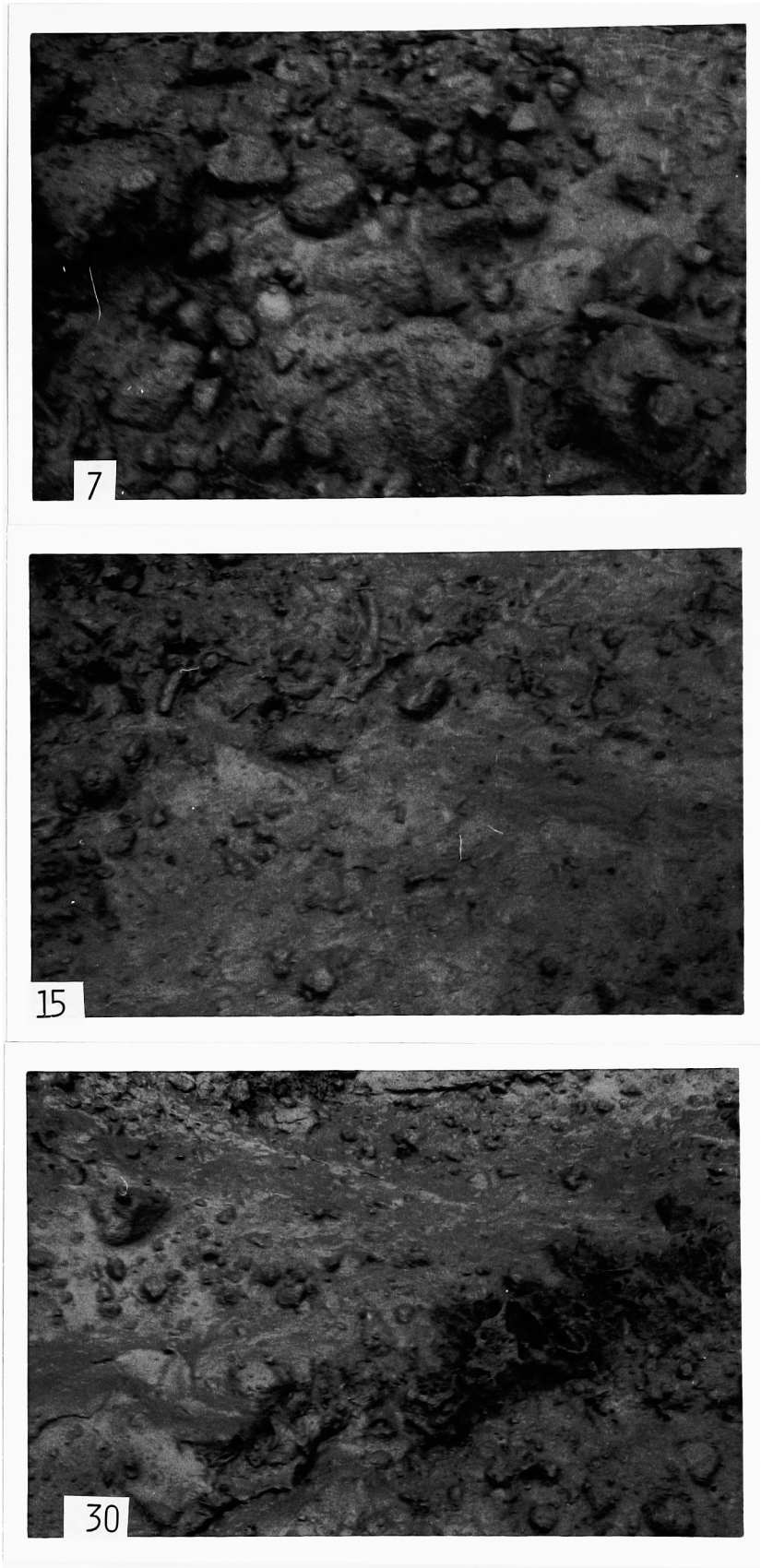

Photo 3. (Continued)

Photo 4. Deposits of different sizes of boulders on the bottom slope in the source area of debris flows at the Kamikamihori valley.

土石流先端への大岩塊の集中機構

諏訪　浩

要　旨

焼岳東斜面の上々堀沢における観測によって、大岩塊が土石流の先端へ集中する現象を定量的に計測した。その結果、これら岩塊のうちの最大級のもののサイズは土石流の流動深とほぼ同程度であることと、最先端部においては集積した石礫の隙間に泥水を欠く部分の存在することを示した。

土石流の中で石礫は大きいものほど浮上しやすいため、浮上してくる大径礫が上層の高流速にのって流送され、土石流の先端へ集まるとの Bagnold (1968) の説明が従来の研究においては定説になっていた。そして、この大径礫の浮上は粒子流における分散圧力または動的篩の効果によって生じると説明されてきた。そこで、筆者は粒状体と水の混合物に振動を加えて動的篩単独の効果を、また剪断を加えて動的篩の効果および分散圧力の効果の片方または複合作用を調べた結果、充分な時間をかけると実験条件によっては大粒径粒子が浮上するため、Inverse grading（逆級化成層）の生じるケースがあるものの、実際の土石流において Inverse grading を形成するほど強力な効果の存在は疑問であることを結論した。いずれにせよ、観測結果によれば、最大級の岩塊のサイズは土石流の流動深と同程度またはそれ以上であり、岩塊は継続的に流路底面に接触しながら転動しているので、その浮上を想定しての先端集中過程の説明は困難である。

そこで、傾斜水路に混合粒径粒子と水を用いて模擬土石流を流下させたところ、大粒径粒子の先端集中が再現されるとともに、大粒径粒子が流れ本体の中へとり込まれ難いという非混入効果の存在することが明らかになった。つぎに、単一粒径の粒子を用いた粒子流においても粒子が同様に先端集中することを示した。これは明らかに Bagnold以来の定説では説明が不可能な現象である。さらに、単一粒子を用いても、粒子が水流段波の先端へ集中したが、その運動は粒径によって異なり、大きい粒子は段波の中にとり込まれた直後はほかの小さい粒子に比べるとやや遅れるものの、すぐに加速して高速度を獲得し、最も早く先端に追いつく

ことを見いだした。

このプロセスについては、石礫にかかる重力の斜面方向の成分と底面摩擦力および流れの抗力の三つの力を考慮した運動モデルによる検討を行った。その結果、谷の上流において一定速度で流下する一様な泥流段波に石礫がとり込まれて動き始める場合を想定すると、石礫はごく短時間で段波の流速より大きな平衡速度に達する。この平衡速度は石礫の粒径が大きいものほど大きくなる特性があり、石礫が大きいほどより早く段波先端に追いつくことを明かにした。

いっぽう、土石流の発生・流下域において谷底に堆積している石礫の転動の起こり易さを検討したところ、一様な定常流に石礫が没しているような状況下では、大きな石礫のほうが転動しやすいことを明らかにした。これは、上位堆積礫の下位堆積礫に対する粒径比が大きいほどピボット角が小さくなるためである。すなわち、堆積物の流動化によって生じる土石流では、その発生・流下過程において大きな粒子から順に流れにとり込まれ易いという一つの基本的な傾向が存在することと、さらに土石流の中で大きな石礫ほど大きな平衡速度を得てより早く流れの先端に追いつくという顕著な特性のあること、また先端に到達した石礫は土石流の先端より先行することができないばかりか、流れ本体の後方へ混入し難いため、土石流先端部には多量の大礫が集積することになることを明らかにした。

このように、上流の急傾斜の谷底において生じる侵食過程では、条件によっては粒径の大きな礫のほうが運搬され易いという一特性のあることが示された。混合砂礫の侵食過程においては、多くの場合、サイズの小さな粒子から掃流され易いので、砂礫の移動限界の研究においてはこのような一般的特性に即した説明がなされている。しかし、条件によっては逆にサイズの大きな粒子から動き易いケースの存在することが分かった。さらに観測では、下流の扇状地などの緩勾配区間においては土石流の減速につれて、大きい石礫からとり残されていくという堆積過程における石礫のソーティングのプロセスが認められるが、この現象についてもそのメカニズムを明らかにした。

キーワード：　土石流、巨礫、先端集中、選択的とり込み、粒度偏析

京都大学防災研究所
〒611京都府宇治市五ケ庄

参 考 論 文　目 次